

NOTE TO USERS

This reproduction is the best copy available.

UMI[®]

Mechanisms of Texture Discrimination: What is Behind the Perceptual
Performance Asymmetry?

François Xavier Sezikeye

A Thesis

In

The Department

Of

Psychology

Presented in Partial Fulfillment of the Requirements

For the Degree of Master in Arts at

Concordia University

Montréal, Québec, Canada.

January, 2005

© François Xavier Sezikeye, 2005.



Library and
Archives Canada

Bibliothèque et
Archives Canada

Published Heritage
Branch

Direction du
Patrimoine de l'édition

395 Wellington Street
Ottawa ON K1A 0N4
Canada

395, rue Wellington
Ottawa ON K1A 0N4
Canada

Your file Votre référence

ISBN: 0-494-04323-7

Our file Notre référence

ISBN: 0-494-04323-7

NOTICE:

The author has granted a non-exclusive license allowing Library and Archives Canada to reproduce, publish, archive, preserve, conserve, communicate to the public by telecommunication or on the Internet, loan, distribute and sell theses worldwide, for commercial or non-commercial purposes, in microform, paper, electronic and/or any other formats.

The author retains copyright ownership and moral rights in this thesis. Neither the thesis nor substantial extracts from it may be printed or otherwise reproduced without the author's permission.

AVIS:

L'auteur a accordé une licence non exclusive permettant à la Bibliothèque et Archives Canada de reproduire, publier, archiver, sauvegarder, conserver, transmettre au public par télécommunication ou par l'Internet, prêter, distribuer et vendre des thèses partout dans le monde, à des fins commerciales ou autres, sur support microforme, papier, électronique et/ou autres formats.

L'auteur conserve la propriété du droit d'auteur et des droits moraux qui protègent cette thèse. Ni la thèse ni des extraits substantiels de celle-ci ne doivent être imprimés ou autrement reproduits sans son autorisation.

In compliance with the Canadian Privacy Act some supporting forms may have been removed from this thesis.

Conformément à la loi canadienne sur la protection de la vie privée, quelques formulaires secondaires ont été enlevés de cette thèse.

While these forms may be included in the document page count, their removal does not represent any loss of content from the thesis.

Bien que ces formulaires aient inclus dans la pagination, il n'y aura aucun contenu manquant.


Canada

ABSTRACT

Mechanisms of Texture Discrimination: What is Behind the Perceptual Performance Asymmetry?

François Xavier Sezikeye

A patch of texture A embedded in a background of texture B, is sometimes detected more easily than a same size patch of texture B embedded in a background of texture A. This phenomenon is called texture discrimination asymmetry. The perceptual texture performance asymmetry was investigated by manipulating the orientation variation of lines, the gradual change of L and + micropatterns and the frequency change in filtered random noise. Variability was shown to be a large contribution in the asymmetry, and a model using quadratic forms and signal detection theory was in qualitative agreement. An experiment with randomly oriented and fixed orientation micropatterns also showed the important role played by variability in asymmetry. The enclosing circles of micropatterns had a contribution lower than variability in asymmetry. The foreground-background area ratio and the textures were important in establishing the way of the asymmetry: classic cases of asymmetry in micropatterns were reversed by manipulating those characteristics. Discrimination, therefore asymmetry, was shown to depend on both edge and region mechanisms.

Acknowledgements

First and foremost, I express my sincere gratitude to my supervisor Rick Gurnsey for his patience and understanding. My gratitude goes also to Sandra Mancini, Cindy Potechin, Sharon Sally, and the other members of the Vision Lab who were always available for my experiments, for their useful comments and encouragement. I would also like to thank my thesis committee members: Michael von Grünau and Michael Bross.

This research was supported by a grant from NSERC awarded to Rick Gurnsey.

Table of Contents

	<u>Page</u>
Chapter 1 Introduction-----	1
1.1 Why Study Texture-----	1
1.2 Asymmetry-----	2
1.3 Models-----	4
1.4 Neural Images-----	8
1.5 Texture Boundaries and Texture Regions-----	15
1.6 Texture Discrimination: Asymmetry-----	16
1.7 Texture Discrimination: Boundaries-----	17
Chapter 2 Signal Detection Theory, Variability and Asymmetry-----	18
2.1 Asymmetry in Texture Perception: The Role of Variability-----	18
2.2 Quadratic Forms in Random Variables-----	21
2.3 Quadratic Forms-----	22
2.4 Computational Methods in Quadratic Forms-----	23
2.5 Experiment 1-----	29
Chapter 3 Textons, Variability and Asymmetry-----	39
3.1 Experiment 2-----	40
3.2 Experiment 3-----	46
3.3 Experiment 4-----	52

Chapter 4 Boundaries, Spatial Frequencies and Asymmetry-----	58
4.1 Discrimination with Abrupt Boundaries-----	58
4.2 Experiment 5-----	59
4.3 Discrimination in Blurry Boundaries-----	66
Chapter 5 General Discussion-----	73
References-----	76

Chapter 1 Introduction.

1.1 Why Study Texture.

Ecological motivations for the study of visual textures rest on the fact that texture, along with size, position, colour, and motion (i.e. the position change rate) is one of the characteristics humans use to correctly categorize objects (Bergen, 1991). Reflectance, coarseness and orientation are texture surface qualities that tell us about the fabric of the visual world and help us segregate different items. Some scientists like Bergen suggest that texture serves as an orienting device for higher visual functions like object recognition. This study concerns how the visual system uses texture.

This study fits among those that address conditions in which texture can be processed by the human visual system quickly (100 ms or less) and effortlessly. In other words, the texture perception of interest is thought to involve preattentive vision, which according to Julesz (1986), operates spontaneously across a wide portion of the visual field, independently of the number of elements.

The visual system can use texture for three purposes: classification, discrimination, and segregation. Classification happens when a subject can sort objects according to their texture, with no direct comparison with other objects. For instance a person identifies a piece of bark as an oak bark because he has seen oak bark in the past or because somebody has described it to him. On the other hand, discrimination implies a certain immediate comparison of two spatially adjacent textures. A depth or material discontinuity can be inferred based on texture differences in neighboring regions. A participant may be unaware of the form of the discriminated object or its boundaries especially if the object is presented very quickly (Wolfson & Landy, 1998).

Lastly, segregation suggests that the object stands out as a unified distinct entity from the background, its form and limits clearly defined. The idea of texture segregation is closely related to the Gestalt notion of grouping. According to the Gestalt psychologists (e.g., Wertheimer, 1923/1958), many small elements, insignificant by themselves, fuse into larger independent significant wholes, that immediately attract attention. However, as to why the segregation or the discrimination happens, the usual Gestalt laws of perceptual organization (i.e., 'good figure', similarity, good continuation, proximity, common fate and familiarity) are considered too vague by present standards.

1.2 Asymmetry

Sometimes, when texture A is embedded in texture B, it is more easily detected than when texture B is embedded in texture A. This phenomenon is referred to as the performance asymmetry. A somewhat coherent theory of texture perception must provide a plausible explanation of the performance asymmetry. Treisman and colleagues (Treisman, 1985; Treisman & Gormican, 1988) were among the first to tackle the asymmetry but within the visual search paradigm i.e., by considering the time it took to find a single item, called target, among many other items different from the target, called distractors. They posited that in order to observe an performance asymmetry, the background (distractors) and the foreground (target) elements should differ at least by one primitive feature whose presence elicited a high level of activity within a so-called "feature map". When the target possessed this feature, search was quicker than when the distractors possessed the feature. So, for the highest performance, it was necessary to have those elements eliciting the lowest activity in the background. Treisman and Gormican (1988)

hypothesized that the asymmetry could be expressed in terms of Weber's fraction (Equation 1.1)

$$\frac{\Delta I}{I} = c \quad 1.1$$

where I is the baseline activity, ΔI is the increment (decrement) and c is a constant. They tested this with vertical lines, the target having a different length than the distractors. When they equated the ratios of lengths in both conditions (long lines in short lines and vice versa), they found no asymmetry.

Gurnsey and Browse (1987, 1989) asked the same question within the texture discrimination paradigm, i.e., a patch of one sort of micropatterns playing the role of foreground against a background made of another sort of micropatterns. One of the variables related to the asymmetry was the size of the minimum enclosing circle of micropatterns composing the textures: larger enclosing circles in the foreground were easier to detect in a background of smaller enclosing circles than the other way around.

Gurnsey and Browse (1989) found a second kind of asymmetry related to the positional variability in the foreground and background: a randomized patch in well ordered rows and columns is more salient than a well ordered patch in a randomized background. Rubenstein and Sagi (1990) also considered variability as a factor contributing to asymmetries. With textures made of L shaped and + shaped micropatterns, they showed that if filtered with Gabors, Ls had more energy variability with rotation than +s, leading to a better detection of Ls in the foreground with +s making the background than +s in Ls.

However, the role of variability was contested by Williams and Julesz (1992a, 1992b) who found that open circles in closed circles would elicit a performance asymmetry even if they presented no variability, i.e., even if all of them had the same orientation. In addition, they contested the Weber fraction law on the basis that it could not predict psychophysical results for arbitrary numbers of targets and distractors. For open circles, Williams and Julesz proposed subjective closedness as a third cause of asymmetry. When presented briefly, a slightly open circle will be seen as closed and a slightly bent line will appear straight. Even two element displays showed asymmetry; the task was to determine if a target was present or not during the trial, half the time it was there, the other half it was replaced by a distractor. Regardless of the case, the open circle was more often misinterpreted than the closed one, so in a background of closed circles, a patch of open circles is less salient than a foreground of closed circles in a background of open circles. Williams and Julesz noted also the necessity to consider the spaces between elements, which they referred to as anti-textons, as a factor in discrimination and asymmetry. With these new tools, they were able to explain reversed performance asymmetry obtained by rearranging space between Ts and Ls: instead of putting a target and distractors in a square grid (display in which L is more salient in Ts than T in Ls), they put them on a circle (T more salient in Ls than L in Ts) in a visual search paradigm. However, Williams and Julesz (1992a, 1992b) did not show how these anti-textons could be applied within a texture discrimination paradigm.

1.3 Models

A good texture discrimination theory should not only correctly predict the psychophysical results in micropattern stimuli, but also apply to natural

textures or to any texture for that matter. In addition, it should be able to explain the many peculiar effects that manifest themselves in different situations, like, to name just a few, the effect of density (Malik & Perona, 1990), the effect of exposure time and the asymmetry effect (Gurnsey & Browse, 1987). Some vision scientists insist that a good model should be consistent with known physiological mechanisms of human vision (Malik & Perona), but other scientists like Marr (1982) think that models can be independent of their physical realizations as long as the predictions are supported by the data. Actually Marr insisted that it was the model that would help understand the physical implementation and not the other way around. Another argument against the need for biological plausibility of a model is the redundant complexity of biological systems (Shanks & Joplin, 1999): many ways might coexist to produce the same end effect. Therefore, even if sometimes it is reported that a model does not exactly use all the pathways that have already been discovered, the best way to falsify it is still to present a case that it cannot predict. The present investigation evaluated especially predictions that different theories make about the asymmetry performance. In addition, this thesis seeks to classify models in two categories: boundary-based and region-based, in order to compare their merits and try to understand what process the visual system is using in processing texture.

Many computational models of texture perception use what Chubb and Landy (1991) called "back pocket models". These models work in three general steps. First, linear shift-invariant, point-wise filters (also called texture grabbers by Chubb and Landy) are applied to texture. This phase is also called feature extraction by du Buf (1992). Second, the resulting image is rectified and thresholded. Rectification is made by taking the absolute value

or square of the filter's output. Thresholding leaves only two values, one for results above the threshold, the other for values below the threshold. This phase corresponds to du Buf's (1992) feature selection phase. Finally, the means of different regions are compared and two regions are said to be distinguishable when their means differ significantly. This is the segmentation phase.

Fogel and Sagi (1989) were among the first to propose this kind of model. They used a quadrature phase pair of Gabor filters as texture grabbers, and summed the squared responses of each pair of filters to obtain a local measure of texture energy. This "energy map" was first smoothed with a Gaussian filter, then followed by thresholding proper and the removal of small islets. Then instead of computing the regional means and comparing them, they applied a Laplacian filter and thus found borders between regions. This model proved to have a high correlation with human performance on micropattern segregation although not all the psychophysical results reported by Kröse (1987) were predictable by the model. In addition, the model could be used on natural textures. However it contained no provisions as to how the performance asymmetry might occur. This model suggested that texture discrimination was done through boundary detection.

Rubenstein and Sagi (1990) attempted to explain performance asymmetries using a variant of the back pocket model. The assumption was that variability within uniformity is more salient than uniformity within variability. Again they illustrated their case using Gabor filters followed by Gaussian blurring, then thresholding and edge detection like in Fogel and Sagi (1989). Then they conducted a statistical evaluation of the model's performance. The spatial variability in filter responses within different

textures was used to compute the difference distribution (means, variances, and noise) at the background-foreground border that was compared to the background-background difference distribution. Rubenstein and Sagi (1990) used signal detection theory to compute the probability of detecting one type of texture in another using the means and variances derived from the model responses. In order to test their theory against psychophysical data published by Gurnsey and Browse (1987), Rubenstein and Sagi took single elements, computed their Gabor filter energies for different orientations and wavelengths, privileged one wavelength to find the mean and the variance for different orientations of the micropatterns, and adjusted the results with a free parameter in order to match human performance. The total correlation value between the model performance and psychophysical results of Gurnsey and Browse (1987) was 0.80, which Rubenstein and Sagi considered very good. Rubenstein and Sagi (1990) also demonstrated empirically that reduction of variability was accompanied by reduction in the discrimination asymmetry. However the Rubenstein and Sagi procedure had a certain number of shortcomings: a) The analysis of individual micropatterns limits the generality of the model; b) Considering only one wavelength is unrealistic because it is likely that many channels contribute to texture discrimination; c) It seemed strange that in the signal detection theory formulae, only the background and the boundary between the background and the foreground were used. According to the last point, this theory, like Fogel and Sagi's, relied on the boundary to explain discrimination.

Not all the models follow the "back pocket model" schema. Several recent papers have tried to answer the criticism that Julesz's (1981) texton theory is based only on imprecise verbal descriptions that have no

computational content. We recall that Julesz described textons as non-overlapping line segments, terminators of line segments, crossings of line segments and blobs with defined length, orientation and width. Julesz posited that these textons were responsible for texture discrimination. Julesz's texton theory was augmented with anti-textons (Williams & Julesz, 1992a, 1992b) which are the space between the textons. Barth and his colleagues (Zetzsche & Barth, 1990; Barth, Zetzsche & Rentschler, 1998) imagined a mechanism that at high spatial frequencies extracted "features" or textons, and at low frequencies gave the results obtained by spatial filters. The former mechanism was called an intrinsic two-dimensional feature detector operator (i2D). The computation consisted of blurring an image with Gaussians, followed by the i2D operators obtained from the eigenvalues of the determinant of the Hessian (partial second derivatives matrix) of the image-intensity function. These operators were able to differentiate two micropatterns that had the same spectral power, in contrast with energy filter models. The i2D model was deemed to simulate the operations done by end-stopped cells, a feat the authors thought out of reach of linear filters such as Gabors even if they were followed by non-linearities. Barth and his colleagues posit that bug detectors in a frog's retina, and the hypercomplex cells in cats and monkeys are perfect illustrations of i2D detectors. This theory seems to be applicable to natural textures and to explain cases where micropatterns with similar inclosing circles are easily discriminated.

The Barth et al. (1998) model contrasts with that of Rubenstein and Sagi (1990) in three ways: a) it does not rely exclusively on energy computations; b) it does not rely on boundary computations; and c) it provides no explanation for the performance asymmetry.

Van Tonder and Ejima (2000a, 2000b) tried to formalize the anti-textons part of Williams and Julesz theory (1992b). In order to characterize space between micropatterns, they created a method that they called the patchwork engine. This algorithm started with boundaries of a micropattern and grew them until they met boundaries of neighboring micropatterns. The last regions to get covered served as centres of new growing regions, and at the same time, they became centres of anti-textons i.e. spaces between micropatterns. Then patches obtained in this way got a weight or luminance equal to average shape differences with the neighboring patches, i.e., a patch very dissimilar to its neighbors got a high value, but similar adjacent patches were assigned a low value. In general tessellation in anti-textons is very different from tessellation in textons. Van Tonder and Ejima linked directly this anti-texton tessellation and weighing to foreground-background asymmetry: in concordance with the Treisman and Gormican (1988) theory, the more active the foreground with respect to the background, the more salient it is, hence the asymmetry. Instead of considering what happened at boundaries as did Rubenstein and Sagi (1990), their method dealt with regions and their patchwork engine accounted for Gurnsey and Browse (1987) results better than Rubenstein and Sagi's without any free parameters. In addition to asymmetry, textons as computed by Barth et al. (1998) and anti-textons as found in van Tonder & Ejima could be used to predict segmentation by following the principle that a gradient in textons and a gradient in anti-textons showed a greater segregation than a gradient in textons alone which in turn was better than an anti-texton gradient alone. Combined with the Barth et. al (1998) theory, the van Tonder and Ejima model applied to natural texture predicted asymmetry but did not use more physiologically plausible

filters like Gabor filters. As to the edge-region classification, this theory clearly used regions in order to find edges, but it was rather a boundary theory of discrimination.

Malik and Perona (1990) invented a clever method to take into account as many visual channels as possible and still avoid the linearity problem. Images were convolved with linear filters. The result of each convolution was half-wave rectified and assigned to an individual "cell". Non-linear inhibition among neighboring cells left only the strongest signals active and these entered the stage of texture gradient computation. Interestingly Malik and Perona eliminated odd-symmetric filters from their first step because odd-symmetric textures offer very poor segmentation. The model predicted satisfactorily Kröse's (1987) and Gurnsey and Browse's (1987) psychophysical data with 96 filters. The model had also the potential to be applied in natural-texture segmentation. All relevant filters could be used because only those with the strongest response contributed to the final result. However the model had no provision for asymmetry performance. The last stage, that is the texture gradient computation put this model in the boundary class.

Liu and Wang (2002) have also implemented a computational texton model using Laplacian, Laplacian of Gaussian and Gabor filters. Instead of using half-wave rectification as did the Malik and Perona model, they tallied pixels of different gray levels in the filtered image for each filter. Two textures that had the same histograms for all filters were deemed perceptually the same. Their model (called the spectral histogram model) was able to predict segregation of many frequently used micropattern textures by looking at differences of texture gradients on either side of a texture border. The larger the difference, the better the segregation. An interesting question with their

model concerns how it might fare in cases of discrimination with diluted edges between textures. Another interesting feature of their theory is that it was able to predict discrimination asymmetries in an elegant manner, with just a few filters (five instead of 96 in the model of Malik and Perona, 1990) and no free parameters. This model accurately predicted human performance (Kröse, 1987), was applicable to natural textures, and explained the asymmetry. It was computationally expensive though. The fact that it was able to discriminate between two non adjacent textures put it in region based theories even if its quantification of the segmentation strength and the asymmetry computation relied first on finding boundaries.

Other researchers were interested in the processes that are in action in digital image processing and in visual perception; they argued that their models do not have to resemble actual cortical processes as long as they give usable results of texture segmentation in vision or in digital image processing. This meant that the mathematical models were not limited to those that were instantiated by known neurons. Some of their challenges were the useful segmentation of radiology and satellite photographs. An example of this approach is seen in the work of du Buf (1992) who used Gabor spectral decomposition with a twist. According to him, authors like Fogel and Sagi (1989) assumed that the visual system knew already where the regions or the boundaries were. Du Buf started with no such assumptions. He computed the local amplitude spectrum at each position of the image obtained by Gabor filters with five frequency bands and six orientation banks. The result was a feature space segmented by a clustering technique called minimum distance pixel classification. However the segmentation that the model produced contained too many sub-regions even if the main regions were correctly

isolated. These subregions were different from the islets found in Rubenstein and Sagi (1990) which corresponded to an activity engendered by texture variability but that texture was still perceived as one entity. On the other hand, du Buf's subregions could be seen as really different textures that our sense of Gestalt included in a larger unit.

Du Buf (1992) also used feature spaces to compute local spectral dissimilarity that resulted in boundary detection: the application of this method gave too many false boundaries making it of little use. A third use of the local Gabor spectrum was to limit the number of parameters to a few semantically meaningful ones like fine-coarse, periodic-aperiodic, isotropic-anisotropic, orientation etc. Every boundary that was found was indeed there but not all the boundaries were found. The last use of the Gabor power spectrum computed its central moments, each moment corresponded to what du Buf called a feature image. The segmentation was obtained by grouping highly correlated moment features: the model gives many subregions, meaning that the boundaries were inaccurate. For du Buf, vision depends heavily on learning, meaning that unsupervised segmentation is unlikely. So texture perception probably uses the minimum distance pixel classification (region based), then it compares the results to known possibilities using the central moments. Du Buf (1992) did not explain the performance asymmetry.

1.4 Neural Images

The study of the neural basis of texture perception has mostly been centered around the measure of neuronal firings in the visual cortex of cats and monkeys. The use of cat and monkey brains seemed appropriate because psychophysical evidence suggests that they show sensitivities with texture contrasts similar to humans (Wilkinson, 1995). The neural activities

associated to texture vision can be traced back to Hubel and Wiesel (1959) and their discovery of cats cortical neurons sensitive to stimulus specific features like orientation. These cells were called feature detectors (Goldstein, 1996), and for those who thought that component features were essential in determining texture, the finding of these feature detectors were the first step in understanding the physiological basis of texture perception.

More recently, Bach and Meigen (1992) found that visual evoked potentials in humans depended on whether oriented lines had all the same direction or were arranged as a checkerboard. Segregation processes elicited specific cortical activities. Those segregation-specific responses were obtained by linearly subtracting signals of pure orientations (vertical or horizontal). Bach and Meigen (1992) suggested that orientation contrast was processed directly and not extracted after different orientations have been detected. In other words, they suspected the existence of boundary detecting mechanisms independent from feature detection mechanisms for the following reason: the visual evoked potential (VEP) corresponding to segregation appeared around 190 ms, a little later than the orientation VEP that appeared at 140 ms but much earlier than the cognitive potentials that peaked around 300 ms. They found that segregation happened too soon after the orientation detection.

With more invasive methods, Nothdurft and colleagues (Kastner, Nothdurft & Pigarev, 1999; Nothdurft, Gallant, Van Essen, 2000) measured directly neuronal responses to texture boundaries. The first paper studied responses in 153 cells in a cat striate cortex stimulated by straight lines. Those lines were surrounded by lines of the same or different orientations outside the classical receptive fields of tested neurons. The mean discharge rates of

these neurons were compared to the firing of a neuron reacting to an isolated line of the preferred orientation. 37 percent of cells showed no change. 33 percent showed a general suppression of firing whether the neighboring lines had the same orientation or different orientation. 22 percent of cells were inhibited but responses to lines with orientation contrast were stronger than responses to same orientation lines. Seven percent of cells showed higher firing in same orientation environment and lower firing in contrast orientation environment. Two percent of cells had a general firing enhancement in same orientation and in contrast orientation. The cells that show sensitivity to orientation contrast may be responsible for pop out phenomena. In the same line of thought, cells that are differentially sensitive to lines surrounded by same orientation lines are good candidates to the detection of uniform textures. Unfortunately, only cells responding to orientation have been tested and it is too early to extend these findings to other features.

In the second paper, Nothdurft, Gallant and Van Essen (2000) looked at the firing of a certain number of striate cortex cells of a macaque monkey. The stimulus was made of homogeneous regions of lines with different orientations that elicited a perception of sharp boundaries between regions in human observers. One of the regions contained preferred orientations for the cells. Here again, the lines were presented in the classical receptive fields of neurons. Responses to optimally oriented lines were higher near texture borders and lower far from the border. Interestingly, the highest response, i.e., the response of cells responding to the border, was about 67% of the activity obtained with a single line alone, suggesting a general inhibition. However, according to Nothdurft, Gallant and Van Essen, these responses

might be enough to allow segmentation, although they suggested at the same time that the discrimination of texture borders might occur at a later stage. In general, inhibitory processes produced by stimuli outside the classical receptive fields of participating neurons may contribute to texture perception.

1.5 Texture Boundaries and Texture Regions

Scholars like Nothdurft (1985) and Landy and Bergen (1991) have defended the idea that discrimination happens because of the structure gradient at texture boundaries. In their model of texture discrimination, Fogel and Sagi (1987) even included as the last step of discrimination, a boundary extractor. Liu and Wang (2002) also computed the gradient differences at the boundary in order to predict discrimination asymmetries. On the other hand, people like Treisman (1985) thought that at the preattentive stage, even if feature maps were retinotopic, the visual system did not retain different locations or boundaries, these locations required attention to be encoded. Gurnsey and Laundry (1992) designed an experiment that showed that performance was only slightly impaired if texture gradients were made smoother. This contradictory research asked whether the visual system extracted first the boundaries in order to discriminate between textures, or vision compared the bulk qualities of different regions and decided if they were different or not. Subsequently, Wolfson and Landy (1998) tried to uncover the mechanisms supporting the boundary-based and the region-based discrimination. They used two textures whose constituent orientations were normally distributed. The textures differed either in the means or the standard deviations of their features about a fixed mean value. In one case, the textures abutted to form a boundary so that boundary discrimination mechanisms as well as region discrimination mechanisms were activated. In

a second case, the two regions were separated by a blank region so that presumably only region mechanisms were in action. Results showed that when textures differed in standard deviation, only region-based mechanisms were at work with similar performance for abutting and non-abutting conditions. In the case of a difference in the mean, edge-based mechanisms were clearly more efficient.

1.6 Texture Discrimination: Asymmetry.

The first question addressed in this thesis concerns the factors that influence performance asymmetry. Researchers have dealt with this question from various points of view as seen above with many examples disproving one or the other theory. Following the idea of Rubenstein and Sagi (1990) that variability was at the origin of the asymmetry, this paradigm was reduced to a simple case of difference in variance in the background and in the foreground, the prediction being that a higher variance in the foreground would lead to a better detection than a higher variance in the background. Two experiments were undertaken: one with oriented lines with a vertical mean orientation drawn from two distributions with different orientation variances. In this case, signal detection theory predicted an asymmetry. The second experiment used two-dimensional random filtered noise for several reasons: when oriented lines are used, the stimulus frame, or the screen frame might have a contribution in the detection of line orientation (Rosenholtz, 2001). Second, the visual system's response to difference in orientation is not uniform, there is a bias towards vertical and horizontal orientations. Third, there is no unfilled space between the micropatterns that corresponds to anti-textons that would make an independent contribution to discrimination. Here the prediction was that, according to the theory of the

minimum enclosing circle (Gurnsey & Browse, 1987, 1989), a low frequency target in a high frequency background would have a better perceptual performance than the opposite case. According to the anti-texton theory, anti-texton absence would eliminate the asymmetry.

Another set of experiments suggested by the Rubenstein and Sagi (1990) theory was that the elimination of orientation variability would lead to the absence of asymmetry. Ls were changed gradually into +s with or without orientation variation. The predictions were that with orientation variation, Ls would be more salient in +s, while no asymmetry would occur with the absence of variation.

1.7 Texture Discrimination: Boundaries.

Except for researchers who were using dissimilarity judgments (Harvey & Gervais, 1978; Gurnsey & Fleet, 2001) to discriminate between textures made of a mixture of different spatial frequencies, many authors used either micropatterns or oriented line segments. For example in the Wolfson and Landy (1998) difference-in-mean experiment, if the mean of one texture was vertical and the other oblique, the fact of seeing one single oblique line might help the observer to conclude that there were two different textures. So, we chose two-dimensional random noise filtered at different frequencies as stimuli. Target areas and perimeters were changed, or the steepness of the boundaries were varied. Predictions were that if texture discrimination was boundary based, the longer the boundary, the more detectable the target, and the steeper the slope, the easier the discrimination. On the other hand if the texture discrimination was region based, the larger the area of the target, the more detectable.

Chapter 2 Signal Detection Theory, Variability and Asymmetry

2.1 Asymmetry in Texture Perception: The Role of Variability

Rubenstein and Sagi (1990) proposed that a texture embedded in a noisy background would be harder to detect than one embedded in a less noisy background. The Rubenstein and Sagi model considered only local differences, therefore it drew a clear boundary between the foreground and the background. In these conditions, the model was one of segregation in which the form of the foreground is known, more than one of discrimination where the acknowledgement of the foreground existence is enough. However, the model is compared to psychophysical data (Gurnsey & Browse, 1987) that were obtained on discrimination tasks. Indeed, Gurnsey and Laundry (1992) showed that large local differences are not necessary to achieve accurate discrimination. Following the idea that noise is related to variability, Rubenstein and Sagi conducted a psychophysical study that demonstrated that the asymmetry in detection of L's in +'s increased with the orientation variability.

The Rubenstein and Sagi (1990) study was based on the signal detection theory (Green & Swets, 1966; Egan, 1975; Falmagne, 1985) which posits that the observer is confronted with two kinds of stimulus: noise (internal and external) and signal plus noise. If we suppose that any stimulus triggers some internal activity, then the response will depend on the activity threshold or criterion one adopts to report that the signal is present. This criterion would depend on some internalized payoff matrix that will not be considered here. The responses can be assigned to four different categories: Misses, when one fails to report signals that are there, Hits when one correctly reports signals, False Alarms, when one reports signals that are not there and Correct

Rejections when one reports correctly that the signal is not there. The lower the activity threshold adopted, the higher the proportions of hits, but also, the higher the proportion of false alarms. This is rendered in the so called Receiver-Operating-Characteristic curve (Figure 2.1) which for a given noise and noise plus signal, will give the probability of hits as a function of the probability of false alarms. The different curves correspond to different levels of signal, which can be deduced from the simultaneous knowledge of the hit rate and the false alarm.

The difference between the noise plus signal and the noise alone (i.e. the level of noise) is called d' (Figure 2.2). When the signal plus noise and the noise are normally distributed, d' is the difference between the means of those distributions divided by the standard deviation of the noise distribution. Independently from the observer, the noise and signal (N+S) curve and the noise (N) curve will determine the probability of correct answer by the following equation, with a as the number of choices the observer has ($a=4$ in a 4AFC). In Equation 2.1, the functions f_N and f_{N+S} can be any density function e.g., normal, chisquare, F or others), P is the proportion correct ((Hits + correct rejection)/total). In a forced choice task chance level performance is equal to $1/a$.

$$P(correct) = \int_{-\infty}^{+\infty} f_N(x) \left[\int_{-\infty}^x f_{N+S}(y) dy \right]^{a-1} dx \quad 2.1$$

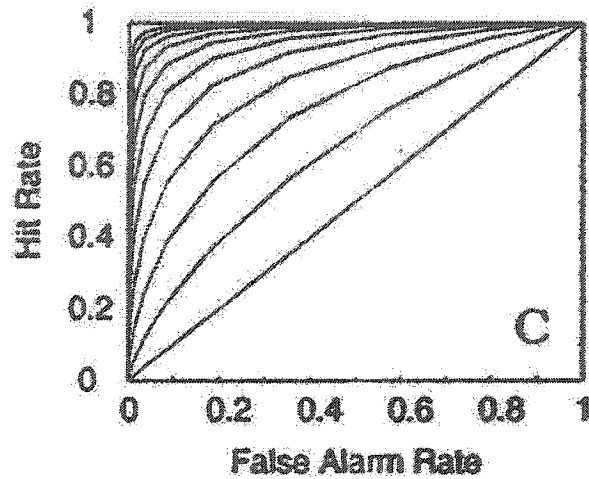


Figure 2.1 Receiver operating characteristic curve. When the participant decides to increase his number of hits, he must be willing to make a higher number of mistakes at the same time, i.e. some of the ambiguous signals he is willing to bet on will reveal to be false alarms.

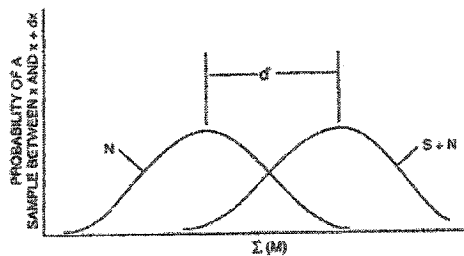


Figure 2.2 Density functions of pure noise and noise + signal. The x-axis is the internal response. Here the signal has as sole effect the shifting of the internal response to higher values. d' is the ratio between the mean difference with respect to the standard deviation of the probability densities.

The Rubenstein and Sagi (1990) paradigm can be simplified in at least two ways: Instead of focusing on variability in filter responses as the origin of the asymmetry, orientation variability in a stimulus can be manipulated. Secondly, a simpler stimulus can be considered. Rather than L's and +'s or other "complex micropatterns," short lines of equal lengths but varying orientations can be used. In this case, the foreground and the background textures may differ in the variability of their components. The orientation of line j would be picked from a normal distribution with variance σ_j^2 and mean μ_j ; a further simplification would take all μ_j 's equal to zero, i.e. all orientations would be randomly distributed about vertical (Wolfson & Landy, 1998). Rubenstein and Sagi based their calculations on the existence of a neat boundary between the noise as a background and the noise + signal as a foreground. However nothing in the signal detection theory presupposes a separation between background and foreground, all that is needed is the expression of noise as a density function and the expression of the noise + signal as another density function. The simplifications suggested above make it possible to characterize those density functions using quadratic forms.

2.2 Quadratic Forms in Random Variables

If we consider a stimulus made of n lines with orientations drawn from n different normal distributions (μ_j, σ_j) , we can calculate quantities that are functions of these orientations, for example, the sum of their squares in degrees S^2 . For a given stimulus, S^2 depends obviously on the mean and the variance of the normal distributions. Some of these new variables have known density functions and cumulative distribution functions and the study of such functions is facilitated by the use of quadratic forms (Mathai &

Provost, 1992). The functions thus found fit perfectly in the paradigm of forced choice in the signal detection theory as used by Rubenstein and Sagi (1990) or Gurnsey and Browse (1987) and can be used to determine if the asymmetry is solely defined by variability (i.e. the noise). If we take again S^2 as an example, for the same number of oriented lines, a region drawn from a single normal distribution will yield a different S^2 than a region made of elements drawn from two distributions.

2.3 Quadratic Forms

Let \mathbf{X} be a real vector made of p real variables, and \mathbf{A} a real matrix,

$$Q = \mathbf{X}'\mathbf{A}\mathbf{X} = \sum_{i=1}^n \sum_{j=1}^n a_{ij}x_i x_j \quad 2.2$$

is a quadratic form in variables x_1, x_2, \dots, x_n and \mathbf{A} is the matrix of the quadratic form Q (Mathai & Provost, 1992). The matrix \mathbf{A} will be assumed to be symmetric in this case.

A quadratic form is said to be positive definite if $\mathbf{X}'\mathbf{A}\mathbf{X} > 0$ for all $\mathbf{X} \neq 0$ and it is said to be positive semidefinite if $\mathbf{X}'\mathbf{A}\mathbf{X} \geq 0$. A symmetric \mathbf{A} has then the following properties:

- i) \mathbf{A} can be written as $\mathbf{P}'\mathbf{P}$ where \mathbf{P} is a matrix of same rank as \mathbf{A}
- ii) The eigenvalues are all nonnegative
- iii) \mathbf{A} has a symmetric square root : $\mathbf{A} = \mathbf{A}^{1/2} \mathbf{A}^{1/2}$

For reasons of expediency in the case of a positive definite matrix, the symmetric square root is replaced by a lower triangular matrix obtained by the Cholesky decomposition:

$$A=T'T.$$

X is said to have a multivariate normal distribution if its probability density function is given by:

$$f(X) = (2\pi)^{-n/2} |\Sigma|^{-0.5} e^{\frac{-(X-\mu)' \Sigma^{-1} (X-\mu)}{2}} \quad 2.3$$

μ is the mean vector of the p normal distributions, and Σ is a $p \times p$ positive definite symmetric matrix that is called the covariance matrix for those distributions. In this case, Q is a linear combination of independent χ^2 variables when $\mu=0$; and of non-central χ^2 variables when $\mu \neq 0$;

2.4 Computational Methods in Quadratic Forms

Several methods have been proposed to find the probability density function and the cumulative distribution function when normal variables can be put in a quadratic form and the normal distributions are known (Mathai & Provost, 1992). Some of these methods can be considered as exact, meaning that the desired functions can be approached with any wanted precision if the calculation tools are powerful enough. These comprise the power series expansions, the Laguerre series expansions and the central χ^2 density expansions. However, these series happen to be computationally expansive and therefore, they are of limited usefulness. As an example, let us analyse the density function as a power series expansion:

$$f(y) = \sum_{k=1}^{\infty} (-1)^k c_k \frac{y^{k-1+p/2}}{\Gamma(k+n/2)}, \quad 0 < y < \infty \quad 2.4$$

p is the dimension of the quadratic form matrix A and it is equal or less than the size of X (number of dimensions). Therefore, the power of y in the numerator of the first term of the series increases with the number of dimension. For p large enough, any somewhat large y will exceed the capacity of any computational device. For our computer (McIntosh G4, 450Mhz, 385M RAM), the power series expansions model should be limited to p inferior to 20 and k around 60 for an error inferior to 0.05 in the cumulative distribution function. Another caveat is to consider λ_i not too different (they are derived from matrix A and covariance matrix Σ in Eq. 2.5 and they enter in the calculations of c_k , large differences in σ_i translate in large differences in λ_i). For a ratio of 1:3, the cumulative distribution in the power series model reaches an error around 0.20 which is unacceptable.

For a higher number of variables, several approximations have been proposed. The simplest one is Patnaik's χ^2 approximation (Mathai & Provost, 1992) in which the quadratic form is equated to a two-parameter χ^2 distribution with the same two first moments i.e. the mean and the variance as the quadratic form.

$$Q=X'AX \approx c\chi_v^2 \tag{2.5}$$

$$\text{with } \sum_{j=1}^p \lambda_j = cv, \quad \sum_{j=1}^p \lambda_j^2 = c^2v$$

where λ_j are the eigenvalues of $\Sigma^{0.5}A\Sigma^{0.5}$. c is a constant and v is the degree of freedom of χ^2 .

A supposedly better approximation is the Pearson approach in which

three moments instead of two are equated (the mean, the variance and the skewness).

$$Q=X'AX \approx \frac{\theta_3}{\theta_2}\chi_v^2 - \frac{\theta_2^2}{\theta_3} + \theta_1 \quad 2.6$$

where $\theta_s = \sum \lambda_j^s (1 + sb_j^2)$; $s=1,2,3$; $v = \theta_2^3 / \theta_3$;

and $\mathbf{b} = \mathbf{P}' \Sigma^{0.5} \boldsymbol{\mu}$.

$$\text{Prob}(Q \leq x) \approx \text{Prob}(\chi_v^2 \leq y) \quad 2.7$$

with $y = (x - \theta_1)\sqrt{v/\theta_2} + v$

Imhof compared the Patnaik and Pearson approximations to exact values for $n=6$ of the cumulative distribution function and found that for an exact value around 0.95, the approximations were less than 0.05 apart. But this does not tell how the approximations would fare for larger p values. Fortunately, it is known that for larger first moments which depend on n , the distribution of Q tends to be a normal distribution (Mathai & Provost, 1992), as does χ^2 .

For large p 's (greater than 150) then, instead of using the normalizing transformation, a simpler way would be to take $E(Q)$ and $\text{Var}(Q)$ as the mean and the variance of the approximating normal distribution. Those two quantities are derived from the first two moments:

$$E(Q) = M_1 = \text{tr} A \Sigma + \boldsymbol{\mu}' A \boldsymbol{\mu}; \quad 2.8$$

$$\text{Var}(Q) = M_2 - M_1^2 = 2\text{tr}(A\Sigma)^2 + 4\mu' A \Sigma A \mu \quad 2.9$$

The use of the quadratic forms in order to find the density functions can be applied in the case of orientation variability in an 4-alternative-forced-choice in which three quadrants have bars oriented according to a given density function that we call noise and the fourth has in addition to noise, some random lines drawn from a different density function, that will be the signal. If variability is important in the discrimination of noise and signal + noise, then the results of the computation will be highly correlated with the human performance. However, we do not expect a perfect correlation because the mechanisms by which the human subject integrates the variability are not taken into account.

Illustration.

Let's take a display made of four quadrants. Three of the four quadrants have $7 \times 7 = 49$ lines whose mean orientation is vertical (0 degree) and whose standard deviation in orientation is 15 degrees. In the remaining quadrant, 40 are drawn from the same distribution as above, and nine are drawn from a normal distribution with the same mean orientation and a standard deviation of 20 degrees (the signal). The sum of the square of the orientations in degrees for each quadrant will obey a χ^2 distribution as approximated by equation 2.6 ($n < 150$) with

$$A = I_{n \times n} \text{ (n \times n identity matrix)}$$

$$\mu = 0_n \text{ (zero vector)}$$

P is a $n \times n$ matrix that diagonalizes $\Sigma^{0.5} A \Sigma^{0.5}$.

$$P \cdot \Sigma^{0.5} A \Sigma^{0.5} P = \begin{pmatrix} I_{4 \times 4} & 0_{4 \times 3} \\ 0_{3 \times 4} & 1.33 \times I_{3 \times 3} \end{pmatrix} \quad 2.10$$

(the standard deviation of the background is normalized to 1)

$$\theta_1 = \Sigma \lambda_i = 52; \theta_2 = \Sigma \lambda_i^2 = 56; \theta_3 = \Sigma \lambda_i^3 = 61.33; v = 46.68$$

combining Equation 2.1 and Equation 2.6 one gets Prob=0.33, above 0.25 which is the chance level. If the signal is in three quadrants, and one is to indicate the quadrant without the signal Prob= 0.31, indicating a slight asymmetry.

If we have a larger display (8x8 lines per quadrant), a larger signal (32 lines out of 64) and a larger standard deviation discrepancy (15 vs 30 instead of 15 vs 20 degrees), the asymmetry is larger P=0.85 and P=0.99 with the quadrant without signal always harder to see than the quadrant with signal (Table 2.1). The asymmetry naturally disappears when all the elements of the three quadrants are drawn from the same distribution (64/64) and all the elements of the fourth quadrant are drawn from a different distribution, because when two quadrants are compared, it is always the same values that are compared (A compared to B or B compared to A) which is a totally symmetrical case, whether A or B constitute the background.

Table 2.1

Signal detection theory simulation with different proportions of signal.

total elements/signal	64/20	64/20	64/32	64/32	64/48	64/48	64/64	64/64
Fg or Bg	Fg=1	Bg=1	Fg=1	Bg=1	Fg=1	Bg=1	Fg=1	Bg=1
1.33	0.38	0.41	0.47	0.50	0.61	0.63	0.74	0.73
1.67	0.47	0.56	0.63	0.72	0.82	0.87	0.95	0.95
2.00	0.53	0.69	0.73	0.86	0.92	0.96	0.99	0.99
2.33	0.58	0.79	0.79	0.93	0.96	0.99	1.00	1.00
2.67	0.61	0.85	0.83	0.97	0.98	1.00	1.00	1.00
3.00	0.61	0.90	0.85	0.99	0.99	1.00	1.00	1.00

Note. Computed asymmetry when the noise (background) and the signal (foreground) are drawn from normal distributions with the same mean = 0; and a different standard deviation. The elements from a more varied distribution are always more salient except when the signal takes all the space.

2.5 Experiment 1.

In the illustration seen above, the use of the signal detection theory on the variability of textures composed of oriented lines shows that there is a perception asymmetry: a foreground of a high variability in a background of lower variability is more salient than a foreground of a lower variability than the background. In order keep as close as possible to the implementation, Experiment 1 uses oriented lines with three quadrants with one variability No (noise) and a fourth quadrant with some lines with variability No and other lines with variability Si (signal). We expect the experiment to validate the illustration results, i.e., if the signal has a higher variability, the fourth quadrant will be more salient than in the case of a lower variability.

Method

Participants

Three graduate students with normal or corrected to normal visions participated in the experiment. Two of them were naive to the purpose of the experiment but all three had been participating in psychophysical experiments with similar stimuli for more than two years.

Stimuli

The stimulus was made of four quadrants of 8x8 elements each. There were seven classes of stimuli representing distributions of straight lines of varying orientation. Within each class the probability of each orientation being presented was determined by sampling from a normal distribution centred at zero degrees with a standard deviation ranging from 2 to 6° in equal logarithmic steps; i.e., 2.00, 2.40, 2.89, 3.46, 4.16, 5.00 and 6°. Each line was drawn in a square 32x32 pixels, its luminance cross-section was a Gaussian with a standard deviation of one pixel.

Two conditions were presented. In the first case, three quadrants contained lines drawn from the distribution having a standard deviation of 2° (D_1). In the remaining quadrant half the elements were drawn from the 2° distribution and half from one of the other distributions (D_2). These D_2 elements were scattered randomly in the quadrant. This corresponded to the general idea of signal in noise. Constructing the stimulus in this way avoided the situation where vertical lines interfere with a vertical boundary by displacing it, thus shrinking or enlarging the signal block by simple illusion (Popple, 2003). Randomization of the signal line positions also minimizes the contribution of external horizontal and vertical lines (such as the boundaries of the computer screen) in the evaluation of the vertical or horizontal boundaries of the target block (Rosenholtz, 2001). The second case was the complement of the first; i.e., D_1 and D_2 switched roles. The task was to find the quadrant that was different. In Figure 2.3, the upper right quadrant contains the disparate region.

Apparatus

Stimulus creation, presentation and data collection were carried out using a McIntosh G4 equipped with a 21 inch Apple Studio Display colour monitor. The monitor was set at a screen resolution of 1600 by 1280 pixels. Each pixel was approximately $0.238 \times 0.238 \text{ mm}^2$. The colour look-up table was calibrated to be linear. The luminance of the gray screen (without stimulus) was equal to 34 cd/m^2 , the black screen was at 0.10 cd/m^2 , and the stimulus had 27.5 cd/m^2 .

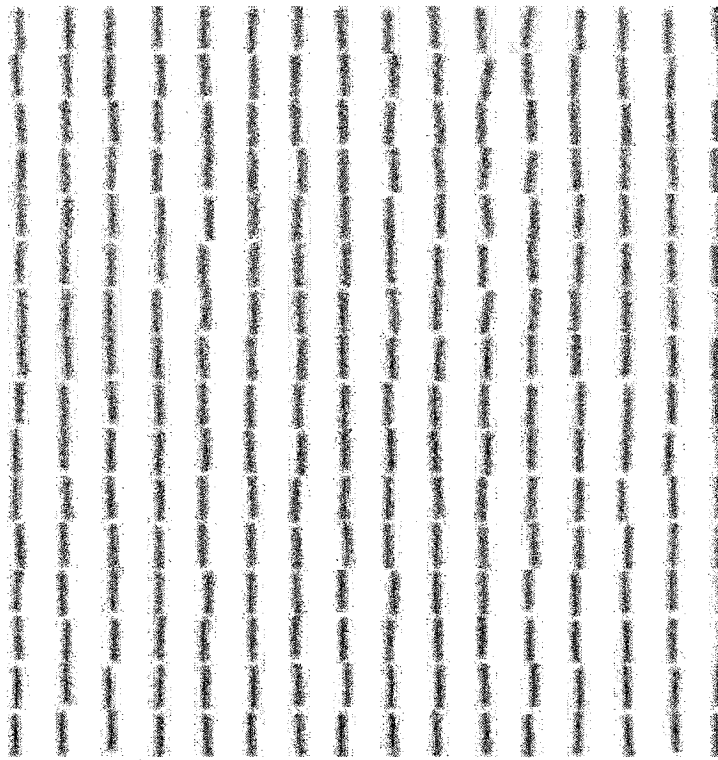


Figure 2.3 Four quadrants with each 8x8 elements. The upper right quadrant has half its lines with an orientation randomly sampled from a normal distribution with a standard deviation equal to 2 degrees around the vertical, whereas the other half is randomly drawn from a normal distribution with a standard deviation equal to 4.16 degrees.

Procedure

Subjects were seated with their eyes 60 centimeters from the screen, and a chin-rest was used to maintain this distance. The stimulus was always centred in the middle of the screen and from a viewing distance of 60 cm the displays subtended 12 x 12 degrees visual angle.

The task was a 4-alternative-forced-choice (4AFC), and on each trial the participant had to indicate the quadrant containing the disparate quadrant by using the numeric keypad; 4 for the upper left quadrant, 5 for the upper right, 1 for the lower left and 2 for the lower right. At the beginning of the experiment, a red fixation point was presented in the middle of a gray screen. The participant was asked to fixate that point before the stimulus was presented. Pressing any key on the keyboard started the experiment proper. After the stimulus presentation, the participant pressed an answer key to indicate his choice, no time limit for the response was set. As soon as one of the answer keys was touched, the next stimulus was presented followed by a gray screen with the red fixation point in the middle.

The foreground/background disparity was determined by the difference in standard deviation between D_1 and D_2 . Seven¹ steps times four quadrants times ten repetitions gave 280 sets that were presented randomly to the participants.

In this and all subsequent experiments, the 4-alternative-forced choice guaranteed a probability to get a hit by chance alone to be $p=0.25$ and the probability to guess wrong to be $q=1-p=0.75$. The number of trials for each condition set at $n=40$ because with a smaller number the probability of getting

¹ The logarithmic scale was chosen because the perception of energy is known to follow geometric progression: when a quantity is squared the participant observes a doubling of the sensation. As the phenomena involved in this study relied in one way or another on energy filters, it seemed more appropriate to use the logarithmic scale instead of the linear one.

above the 72 percent threshold by chance alone or by mistake would be too large. On the other hand, a larger number of trials, say one hundred, would make the experiment longer for participants, but the results would be more reliable. The number of 40 seemed a good balance because it was short enough for participants (around five minutes for 40 trials times 7 steps) and the following calculations show that if the threshold was fixed at more than 70 percent correct, $n=40$ was a comfortable number for probability purposes. Zar (1984) gives the calculations to decide if that value is in the confidence limits (95 percent confidence interval in our case) for a binomial distribution such as ours.

The lower confidence limit is given by:

$$L_1 = \frac{X}{X + v_1 F_{\alpha, 2v_1, 2v_2}}, \quad 2.11$$

with $v_1 = n - X + 1$, $v_2 = X$, $X = pn$

The upper limit is

$$L_2 = \frac{F}{n - X + F}, \quad 2.12$$

with $F = (X + 1)F_{\alpha, 2v_1', 2v_2'}$, $v_1' = v_2 + 1$, $v_2' = v_1 - 1$.

The null hypothesis was that 28 hits out of 40 (70 percent hits) could be obtained with $p \leq 0.25$ by chance alone (in the 95 percent confidence interval)

$$H_0: p \leq 0.25; \quad H_1: p > 0.25 \quad 2.13$$

$$X = pn = 0.25 \times 40 = 10,$$

$$n'_1=10+1=11,$$

$$n'_2=40-10+1-1=30,$$

$$F'=(10+1)F_{0.05(1),22,60} = 11 \times 1.72 = 18.92,$$

$L2=18.92/(40-10+18.92)=18.92/48.92=0.387 < 0.70$. At 70 percent or more hits threshold we can comfortably reject the null hypothesis (of chance performance) with 40 trials: such a high hit rate does not happen by chance alone.

As a consequence of the large number of trials we did for each condition, just a few participants were required to make most of the experiments. This follows a long tradition of psychophysical studies where sometimes only two participants were reported, the second participant being there to ascertain that the phenomenon studied did not show idiosyncratic results.

Results

The raw and average data are reported in Figure 2.4. All three participants found it easier to detect a high variation quadrant among low variation quadrants than a low variation quadrant among high variation quadrants almost all the time (Figure 2.4). Thresholds were found by fitting the data with a Weibull function (Figure 2.4). The results of the curve fitting are shown in Table 2.2. Column (a) gives the standard deviation threshold, column (b) gives the second parameter of the Weibull function that is the steepness at threshold, and the r^2 column gives the the variance of the data explained by the Weibull function fitting curve. The Weibull function was chosen as the fitting function because it is known to fit best psychophysical data (Harvey, 1986). The 72 percent threshold was obtained at a foreground orientation standard deviation 2.17 times larger than that of the background.

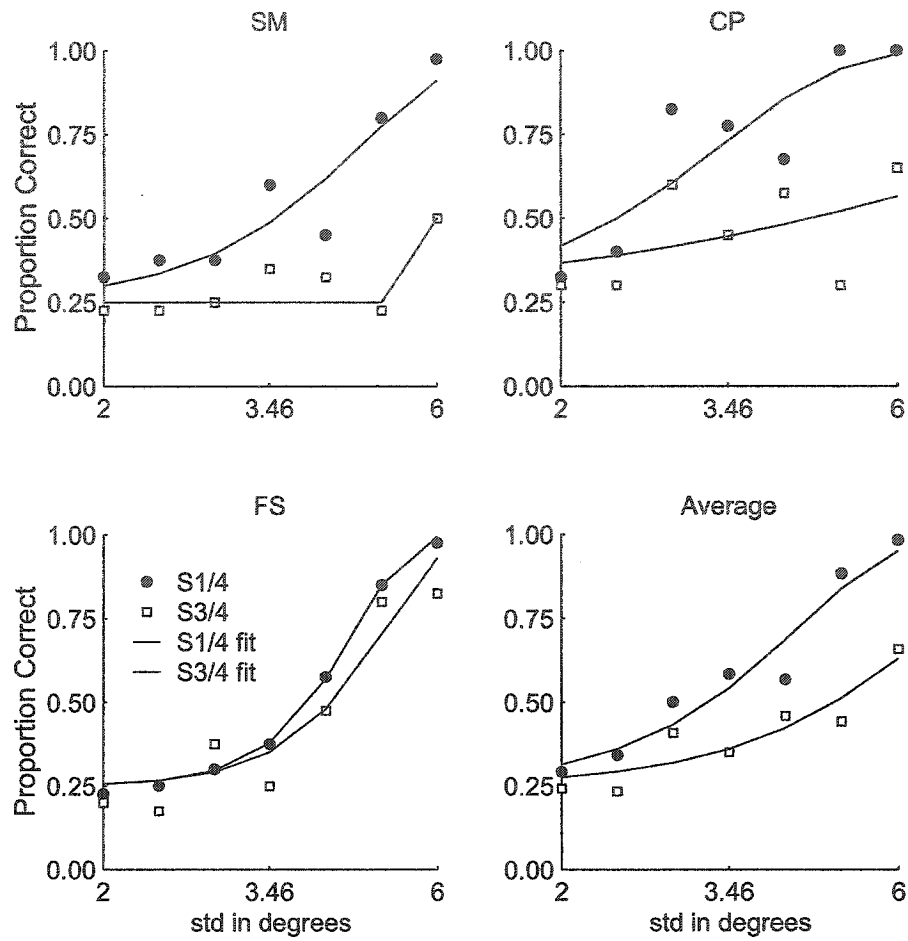


Figure 2.4 Results for three participants and their average. The x-axis was the orientation standard deviation, starting from the lowest standard deviation (two degrees). The other values were obtained by taking seven logarithmic steps from two to six. Only one quadrant had the high variability in S1/4 and three quadrants had the high variability in S3/4. One quadrant with more variability (S1/4) was more salient in a background with less variability than one quadrant with less variability (S3/4), i.e., the threshold was reached at a smaller orientation variation.

Table 2.2.

Discrimination thresholds (72% correct) of oriented lines drawn from two normal distribution variations around vertical direction.

	A in one quadrant			A in three quadrants		
	a	b	r^2	a	b	r^2
SM	2.36	3.14	0.86	3.02	1.44	0.74
CP	1.72	2.55	0.76	5.29	1.07	0.24
FS	2.30	5.88	1.00	2.53	5.10	0.90
Average	2.17	3.10	0.94	3.40	2.74	0.85

Note. A is the stimulus with the highest variance, a is the threshold, b is the steepness and r is the variance explained by the fitting Weibull. The average reported here is the fitting on the average of raw data.

When the background standard deviation was larger, the extrapolation to 72 percent correct rate was 3.40 larger than the foreground standard deviation. The thresholds showed the same asymmetry in the same direction for all participants. The thresholds in the case of one quadrant with a lower standard deviation than three others are out of the measured data resulting in a poor fit. It's clearly difficult to detect a "low variance" stimulus embedded in a "high variance" background. That was especially true for subject CP whose threshold in the hard condition was so high that the variance explained by the fitting curve was mediocre (0.24).

Discussion

All three subjects showed asymmetry in the sense predicted by the quadratic forms implementations but not of the same magnitude. The experiment corresponded to the computed case 64/32 in table 3.1. (64 lines, 32 of them with the foreground orientation). Instead of 2.15 and 3.40 ratios found in the experiment, the model gives 1.67 and 2. The disparity between the experimental results and the calculations might stem from the blindness of the latter to the non linearities of the visual system. It is known that the perception of vertical lines is more efficient than that of oblique lines, but there is no such provision in the model: all that is taken into account is the ratio between the variation of the signal and the variation of the background. In addition the ceiling is easier to reach in the psychophysical experiment. To the question whether the addition of a free parameter in the computational model might bring its performance into line with the psychophysical results, the answer is maybe. We took the psychophysical data only for one setting (64 lines, 32 with a different orientation variance).

In order to complete the model we would have to make experiments with different settings. This would include, with an eventual free parameter, a variable for the foreground-background lines, the line density, etc...

Nonetheless, the main conclusion is that Rubenstein and Sagi (1990), may have a point, the variability of the stimuli is important for the perception of an asymmetry between a background and a foreground. The noisier the background, the more difficult it is to notice a flatter foreground. However it remains to be seen if that variability is the only factor or even the most important factor for asymmetric salience.

Chapter 3 Textons, Variability and Asymmetry

Gurnsey and Browse (1987) found that randomly rotated Ls are more easily detected when embedded in randomly rotated +s than vice versa. In their paradigm stimulus presentation time was varied from 67 to 167 ms and the stimulus was followed by a 500 ms mask. Ls and +s were always randomly oriented and jittered in order to reduce the help of global alignment.

Rubenstein and Sagi (1990) tested the assumption that variability was the main cause of asymmetry. In a four-alternative-forced-choice (4AFC) paradigm, they embedded a 3x3 matrix of Ls in a 15x15 matrix of +s in different rotations of the micropatterns (one, two and many), or they embedded +s in Ls. By varying the inter-stimulus interval (the interval between the stimulus and the mask) they found an asymmetry only when there was a high degree of orientation variability (i.e. not in the cases of 1 and 2 orientations).

The present study was conducted in an attempt to replicate the Rubenstein and Sagi (1990) results using a different paradigm. Rather than limiting performance by varying exposure duration, a continuum of texture elements was created that ranged from X-type to L-type micropatterns. Figures 3.1 and 3.2 give examples of such micropatterns.

The general settings of Experiment 2 were essentially the same as in Experiment 1. The task was a Four-alternative-forced-choice (4AFC) with seven logarithmic steps of the independent variable. Data fitting and the thresholds at 72 percent correct were found using Weibull fitting functions and the predictions were stated in terms of thresholds.

We predicted that in the case of random variation, the results would be similar to Gurnsey and Browse's and Rubenstein and Sagi's, i.e. Ls would be



Figure 3.1 Micropatterns changing from rotated L (V) to rotated + (X) in seven logarithmic steps (from left to right $a = 0,1 \ 0,15 \ 0,22 \ 0,32 \ 0,46 \ 0,68$ and $1,0$)

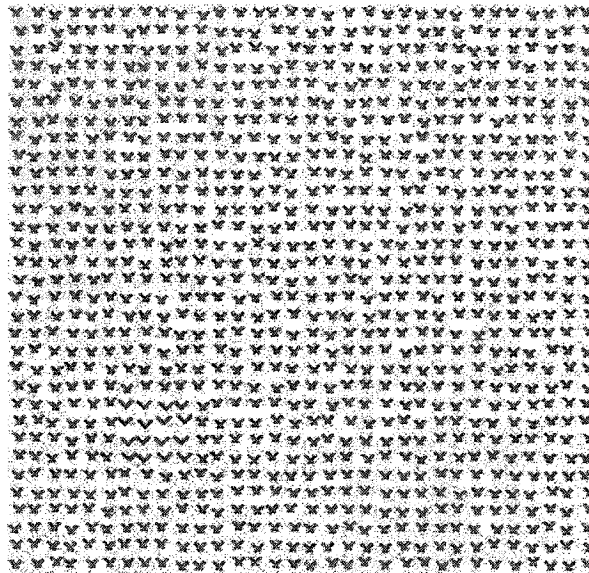


Figure 3.2 Vs (Ls rotated by 45 degrees) in Xs (+s rotated by 45 degrees). The background varies in seven logarithmic values from Vs. Vs and Xs are preferred to Ls and +s in order to attenuate vertical borders effects (Rosenholtz, 2001; Popple, 2003). In the other case, Vs are in the background and the foreground is varied, a perfectly symmetrical situation to the shown stimulus. $a = .6$

seen more easily among transformed Ls (lower thresholds) than transformed Ls among Ls. However, in the absence of orientation variation, Rubenstein and Sagi's theory would predict an absence of asymmetry whereas Gurnsey and Browse (1989) would still predict an asymmetry due to the difference between the inclosing circles for Ls and transformed Ls.

3.1 Experiment 2

Method

Participants

Three Concordia University graduate students with normal or corrected to normal vision participated in the experiment. One participant was naive to the purpose of the experiment and the other two had participated in similar experiments in the past.

Stimuli

The stimulus was shown in four quadrants. Three of the four quadrants comprised only one type of 16x16 micropatterns and the fourth contained a six by six region of different micropatterns. The foreground was made of the other sort of micropatterns. One of the textures was always made of Ls, and the other texture changed from Ls to +s in seven logarithmic translation steps ($a = 0.00 \ 0.13 \ 0.18 \ 0.24 \ 0.33 \ 0.45 \ 0.60$); $a=0.0$ produces an L and $a=1$ produces a + (Figure 3.1). The values between those extremes gave micropatterns resembling Ls with shorter lower branches. Figure 3.2 , Figure 3.3 and Figure 3.4 show cases in which $a = 0.60$. In Figure 3.2 and Figure 3.3 Ls are embedded in +s and in Figure 3.4 +s are embedded in Ls. Four conditions were run: in the first two conditions all Ls and +s were rotated by 45 degrees (Vs and Xs all oriented upwards). In the first condition, Vs were embedded in Xs and in the

second condition Xs were embedded in Vs. Vs and Xs were chosen instead of Ls and +s because the oblique lines would not interfere with the vertical (or horizontal) boundaries of the background (Poppo, 2003; Rosenholtz, 2001). In the two last conditions, Ls and +s were randomly oriented; but again in one condition Ls were embedded in +s and in the last one +s were embedded in Ls.

Procedure

The procedure was identical in most respects to that of Experiment 1. except the distance between the eyes and the stimulus was 120 cm instead of 60 cm. The number of the trials was the same

Results

The data of each subject and the average data are shown in Figure 3.5 . The ratio change values vary from zero (uniform texture) to one (maximal difference). When there is no orientation variation the curves are quite similar independently of the texture in the foreground. When the micropatterns are randomly oriented the detection of the +s foreground never exceeds chance level. All data were fit with Weibull functions to obtain the 72 percent threshold values and the results are shown in Table 3.1. We have too few subjects to get significant statistics on variability ($F(1,2)= 1.42$, $p=0.35$) or foreground ($F(1,2)=1.59$, $p=0.33$) but all of them agreed that they saw the foreground in only three of the four cases. In the fourth case, they saw nothing and the corresponding curves are so flat for the fourth condition (+in L) of Figure 3.5 that the thresholds make no sense.

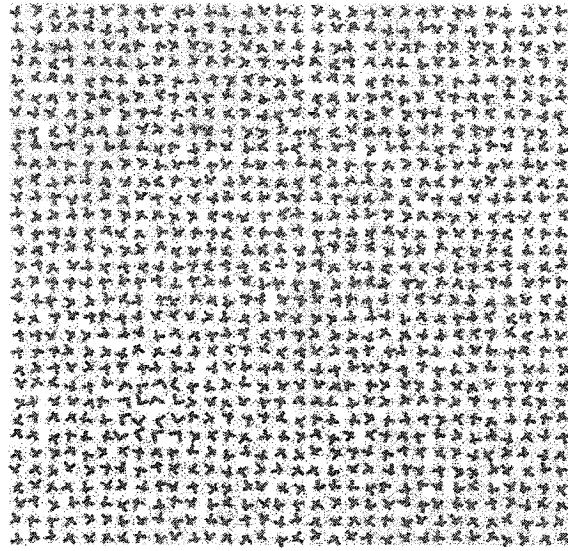


Figure 3.3 Ls in +s in random orientations. In this case, Ls are in the background and altered Ls (or +s) were in the foreground. Here too, a is equal to 0.60.

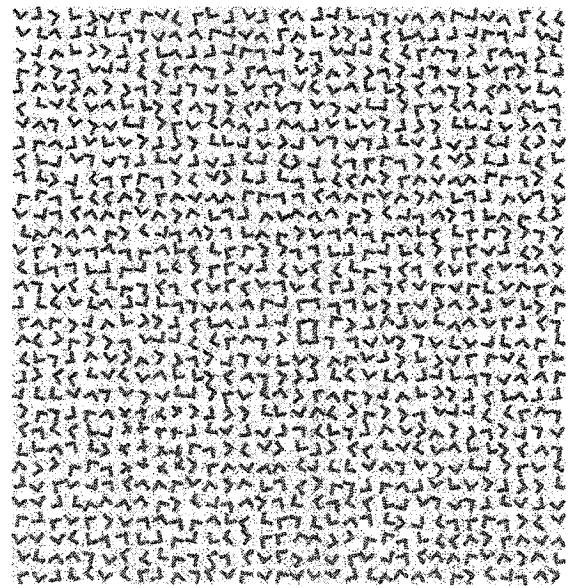


Figure 3.4 +s in Ls in random orientations: symmetrical case of Figure 3.3.

Table 3.1

72 percent Weibull threshold for three participants and slopes at threshold. Full Ls (or Vs) were always present^a.

Threshold (first Weibull argument)				
	V in X	X in V	L in +	+ in
DH	0.39	0.61	0.45	0.99
FS	0.46	0.59	0.47	5.43 ^b
KM	0.49	0.44	0.47	0.61
mean	0.44	0.55	0.46	0.61
slope (second Weibull argument)				
	V in X	X in V	L in +	+ in L
DH	3.83	3.88	4.72	2.92
FS	4.97	2.84	3.41	16.98
KM	4.12	3.27	2.54	95.13
mean	4.97	2.92	3.34	85.85

^aNote: zero corresponded to full Ls and one related to full +s, so only the +s (Xs) varied.

^bNote: The curve is so flat that the threshold is meaningless.

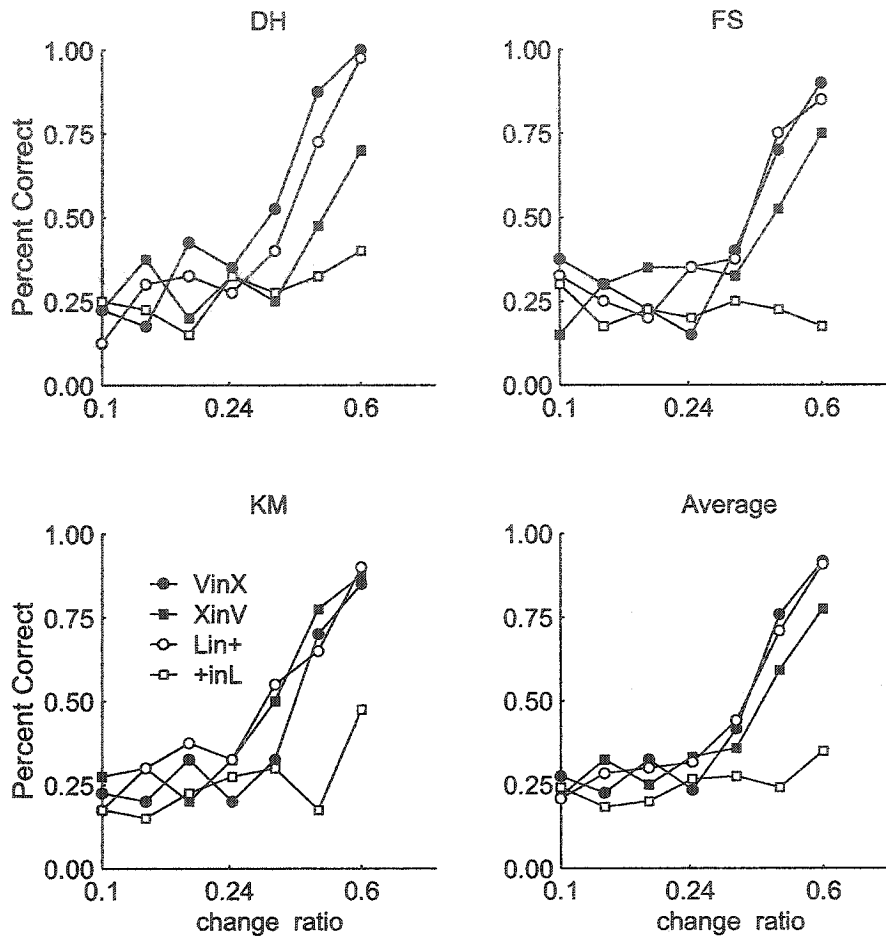


Figure 3.5 Results for three participants. Random +s are hard to perceive in random Ls for all participants. The ratio change stopped at 0.6 because there was no need to go further, most participants had reached the ceiling for some stimuli.

Discussion

This experiment was motivated by Rubenstein and Sagi's (1990) assumption that variability was a major cause of perceptual asymmetry. Without orientation variation only a slight asymmetry was found which was not statistically significant because of the size of the sample. However, when orientation variability was added the asymmetry was so strong that all participants reported low discrimination. Thus variability makes an important contribution to texture perception asymmetry. However the influence of the enclosing circles is weaker because in both cases (with variation and without variation) the enclosing circles are larger for Ls than for +s but the asymmetry in the absence of variation was marginal. Ls in +s were more salient than +s in Ls as reported by Gurnsey and Browse (1987, 1989) only in the case of orientation variation. In order to investigate further the effect of parameters other than variation, the number of elements shown in the stimulus was varied in the following experiment.

3.2 Experiment 3.

In this experiment the stimulus has the same size but the micropattern size is doubled and the foreground was a fourth of the quadrant's size. This should show the effect of micropattern density.

Method

Participants

Six Concordia University students with normal or corrected to normal vision participated in the experiment. Four of them were naive to the purpose of the experiment and two had participated in similar experiments in the past.

Stimuli

As in Experiment 2 the stimulus was made of four quadrants but this time instead of 16x16 micropatterns of 32x32 pixels the stimulus was made of 8x8 micropatterns covering 64x64 pixels each. The foreground was made of four by four micropatterns in the middle of the target quadrant (Figure 3.6 and Figure 3.7). The stimulus was viewed at a distance of 120 cm as before for the same visual angle.

Procedure

The procedure was identical to that of Experiment 2.

Results

The results are shown in Table 3.2. and Figure 3.8. All participants showed an asymmetry in the same sense, i.e. +s in Ls had lower thresholds than Ls in +s, that is, +s in Ls were more salient than Ls in +s. The reverse results were expected, i.e., Ls in +s were supposed to have a lower threshold. The foreground texture main effect was significant, $F(1,5)=46.92$, $p=.001$: the +s in Ls threshold was statistically lower than Ls in +s threshold (Appendix 1). There was another main effect of orientation, $F(1,5)=9.06$, $p=.03$, meaning that the stimulus with randomly oriented micropatterns was more difficult to discriminate. However the interaction between the foreground and the randomness was not statistically significant, $F(1,5) = .056$, $p= .82$.

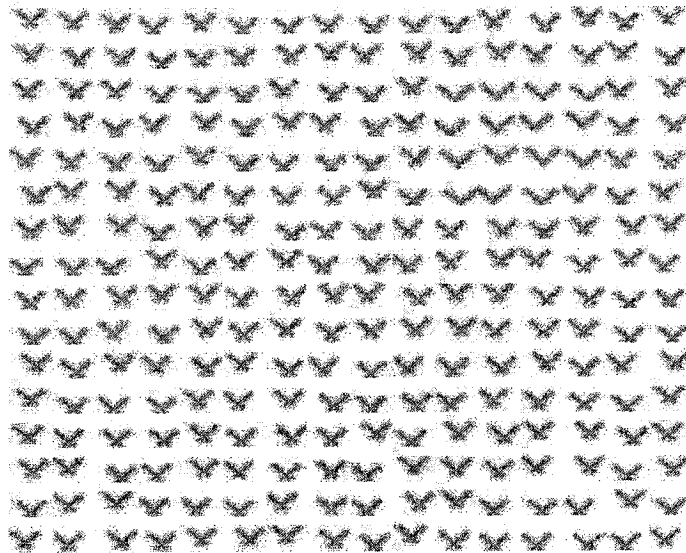


Figure 3.6 Vs (Ls rotated by 45 degrees) in Xs (+s rotated by 45 degrees). The foreground takes a quarter the area of the quadrant

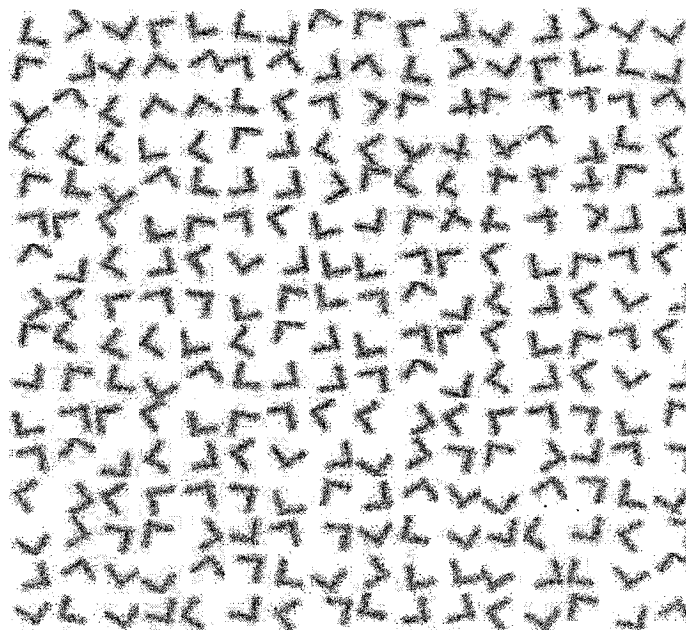


Figure 3.7 Ls in +s in random orientations. a was equal to .464.

Table 3.2

72 percent thresholds with Ls and +s randomly oriented or not, Ls or +s in the foreground. Ls were the fixed micropatterns.

Participants	one orientation		random orientation	
	Vs in Xs	Xs in Vs	Ls in +s	+s in Ls
AP	0.57	0.47	0.66	0.53
SM	0.49	0.28	0.45	0.33
CP	0.43	0.31	0.55	0.46
XS	0.46	0.38	0.50	0.39
MA	0.59	0.31	0.58	0.41
NW	0.47	0.41	0.58	0.40
mean	0.50	0.36	0.55	0.42
SEM	0.06	0.07	0.08	0.07

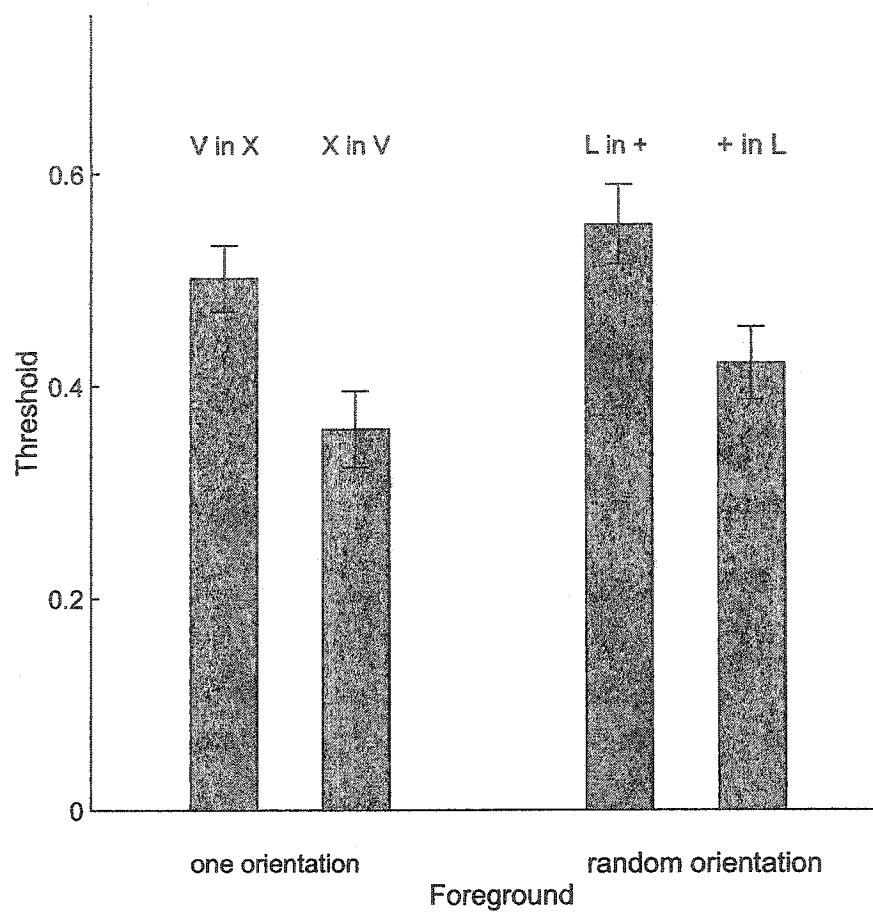


Figure 3.8 Thresholds at which the foreground was seen 72 percent of the time in Experiment 3. +s in Ls are more salient.

Discussion

When Ls and +s textures were directly compared in Experiment 2 (and Gurnsey and Browse (1987,1989) and Rubenstein and Sagi (1990)), Ls in +s background were more salient than +s in Ls. But in this experiment, half-way +s in Ls were more salient than Ls in half-way +s, the first having systematically lower thresholds than the second (Table 3.2). This reversal of asymmetry begs for a new explanation for asymmetry because the traditional explanations based on size or positional variability (Gurnsey & Browse, 1989) are insufficient. In the present experiment, the micropatterns with the largest enclosing circles were less salient.

From the Gurnsey and Browse seminal papers in 1987, situations have changed, textons got new champions who proposed computational methods to quantify them (Barth et al. 1998). If the textons were to play a role in the asymmetry, then the difference between textons of Ls and +s might explain the asymmetry and lead to further predictions. The reversal of perceptual asymmetry is similar to the one reported by Williams and Julesz (1992a, 1992b) and might have the same causes. There are two main differences between Experiment 3 and Experiment 2. First the micropatterns are twice as large in Experiment 3 compared to Experiment 2, so the textures engage lower frequency mechanisms. Furthermore, micropatterns may be perceived individually instead of fusing into a coherent patch, thus making a difference in asymmetry. The second difference is the ratio between foreground and background areas. In Experiment 3 the ratio was 33 percent and in Experiment 2 the ratio was 16 percent. This difference may be important in the expression of asymmetry too. One of Williams and Julesz's (1992b) explanations of asymmetry was that one of the textures might be easier to transform into

another than the other way round and that the visual system was trying to standardize all micropatterns. A few easily transformable micropatterns would disappear in a sea of more stable micropatterns (a few slightly bent lines in a sea of straight lines will be hard to see). If the foreground is proportionally more important, the job might be harder, hence the asymmetry reversal. The features that were easy to transform might be more difficult now. In order to explore the influence of micropattern characteristics Experiment 3 was modified and instead of full Ls and variable +s, one of the textures was made of full +s and variable Ls. The motivation behind this change was that full +s have always the same features as variable Ls (line crossings) whereas full Ls (elbows) are very different from variable +s (line crossings).

3.3 Experiment 4.

Method

Participants

Four Concordia University graduate students with normal or corrected to normal vision participated in the experiment. All of them were familiar with the procedure and the visual stimuli but they were naive to the purpose of the experiment. All of them had participated in experiment 3.

Stimulus

The stimulus was similar to the stimulus of Experiment 3 with the exception of the basic micropatterns which were +s instead of Ls. So one texture was always made of complete +s the other texture micropatterns would vary from +s to Ls in logarithmic steps (Figure 3.9). As the variation ratio a never exceeds 0.6, full Ls are never shown but full + are always present. Another condition was fixed versus random orientation.

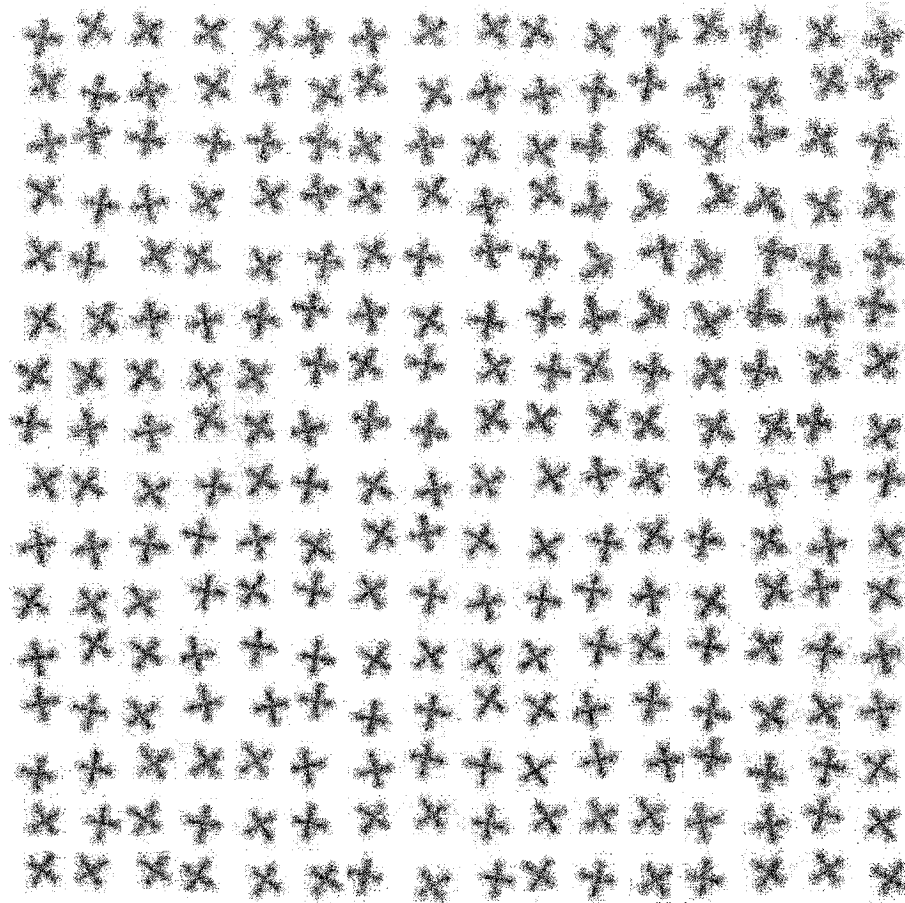


Figure 3.9 Ls (altered +s) foreground in a +s texture background as shown in Experiment 4. In two settings, the micropatterns were oriented randomly (stimulus shown above) and in two other settings, the Ls and the +s had all the same direction (rotated by 45 degrees).

Procedure

The procedure was identical to that of Experiments 2 and 3.

Results

The results of the four participants are illustrated in Table 3.3 and Figure 3.10. For all subjects and in all orientation conditions, Ls in +s were systematically more salient than +s in Ls as the thresholds were always lower. These results conform with the classical case. The main effect of the texture in the foreground was significant, $F(1,3)=41.88$, $p=.007$: the Ls in +s threshold was statistically lower than +s in Ls threshold (Appendix 1). There was also a main effect of orientation, $F(1,3)=49.78$, $p=.006$, the stimulus being more difficult to discriminate with micropatterns oriented randomly. However the interaction between the foreground and the randomness was not statistically significant, $F(1,3) = .32$, $p= .61$.

Discussion

When we considered +s in altered +s (Ls) and altered +s (Ls) in +s, we got the classic case reported by Gurnsey and Browse (1987) where Ls (altered +s) in +s are more salient. Even the effect of variability was slightly positive. The results to this point may be summarized as follows: There was something different between Ls and altered Ls that could not be found between +s and altered +s in that the asymmetries were not shown in the same direction when the stimuli were shown with the same stimulus onset asynchrony. That something might be the texton differences: the crossings in altered Ls were showing more activity than the elbows of full Ls. However when full Ls were compared to full +s, the influence of the minimal enclosing circles overcame the influence of the textons. In other words if +s were enlarged

Table 3.3

72 percent thresholds with Ls and +s randomly oriented or not, Ls or +s in the foreground

Participants	one orientation		random orientation	
	Vs in Xs	Xs in Vs	Ls in +s	+s in Ls
SM	0.23	0.32	0.29	0.38
CP	0.20	0.37	0.35	0.41
NW	0.32	0.35	0.32	0.60
MI	0.20	0.37	0.28	0.48
mean	0.24	0.35	0.31	0.47
SEM	0.06	0.02	0.03	0.10

^aNote: zero corresponds to full +s and one corresponds to full +L, so in the stimulus full +s were always present.

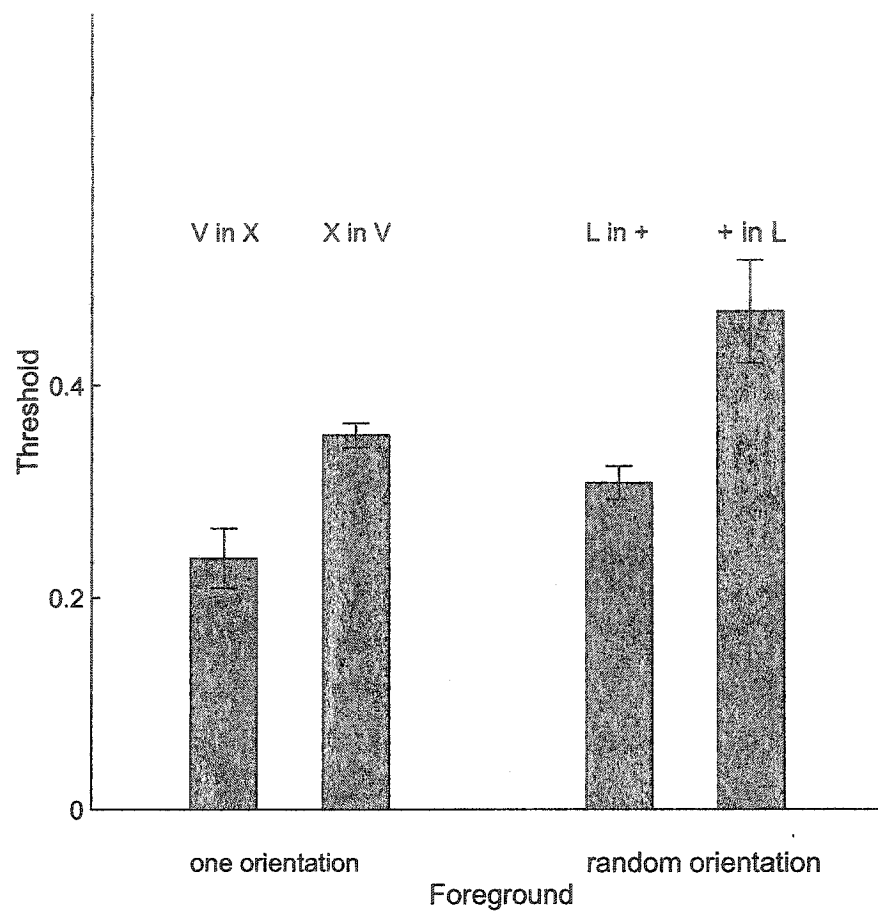


Figure 3.10 Results when X are constant and the other micropatterns are variations of X. The results are opposite to those reported on Figure 3.8.

gradually while Ls were constant, they got to the point where they did not present a perceptual asymmetry. However, one might bear in mind that the disappearance of asymmetry does not go hand in hand with the disappearance of discrimination, as Barth, Zetzsche & Rentschler (1998) have shown that textons contributed more heavily in discrimination than the size of the enclosing circles.

Experiment 2 confirmed Rubenstein and Sagi's (1990) assumption that variability contributes to asymmetry. Gurnsey and Browse (1989) showed that enclosing circles also contribute to asymmetry. Experiments 3 and 4 ascertained that features that Williams and Julesz (1992a, 1992b) called textons and anti-textons are also important to asymmetry. Asymmetry therefore depends on many attributes that may enhance each other or act in competition.

Chapter 4 Boundaries, Spatial Frequencies and Asymmetry

4.1 Discrimination With Abrupt Boundaries

In their 1990 paper, Rubenstein and Sagi studied the asymmetry by considering what happened at the boundaries of disparate regions. Several studies have shown that texture discrimination is affected by the “sharpness” of local texture gradients; the more abrupt the transition the easier the discrimination (Nothdurft, 1985; Landy & Bergen, 1991; Gurnsey & Laundry, 1992; Wolfson & Landy, 1998).

An alternative view is that texture discrimination is “region based,” meaning that sensitivity to texture difference is not significantly affected by the proximity of the two textures involved, or the sharpness of edges that separate them (Gurnsey & Laundry, 1992; Wolfson & Landy, 1998; Gurnsey & Fleet, 2001). The experiments in this chapter were designed to test if region properties or edge properties were more important to texture discrimination, and if the asymmetry was also influenced. We made the following assumptions (Seizikeye & Gurnsey, 2003):

1. Increasing the number of edge locations should improve performance, and the asymmetry if discrimination is based on edge-sensitive mechanisms.
2. Increasing the spatial extent of a disparate texture region should improve performance and the asymmetry if discrimination is based on region-sensitive mechanisms.

We used filtered random noise. An advantage of this kind of stimulus was that the influence of direction was minimized by the suppression of rows and columns, the foreground-background edges were round, preventing the influence of diverse vertical and horizontal contours such as the borders of

the stimulus and screen (Rosenholtz, 2001; Popple, 2003). We avoided using micropatterns also because different micropatterns might engage many different mechanisms. In this case, the same mechanism is supposed to be at play but on different scales. In addition, the random noise stimulus might help replicate the results obtained by Gurnsey and Browse (1989) with circles of different sizes; i.e., that large circles in small circles were more salient than small circles in large ones. In the language of spatial frequency analysis low spatial frequency noise in high spatial frequency noise should be more salient than high spatial frequency noise in low spatial frequency.

Experiment 5

Method

Subjects.

Nine participants were selected from the Psychology department at Concordia University. All reported normal to corrected-to-normal vision.

Stimuli.

Stimuli comprised circular (single edge) and annular (double edge) texture regions embedded in larger backgrounds (Figure 4.1). The circular texture region was 33% larger than the annular one, but the annular texture region boundary was 50% longer. If edge information is the main factor used in discriminating textures, then the annular regions should be detected more easily than the circular regions.

Stimuli were created from seven random noise textures filtered with frequencies ranging from 3.65 to 4.74 cpd in equal log steps. All textures had the same mean luminance (39.8 cd/m²) and contrast. Stimuli were created by

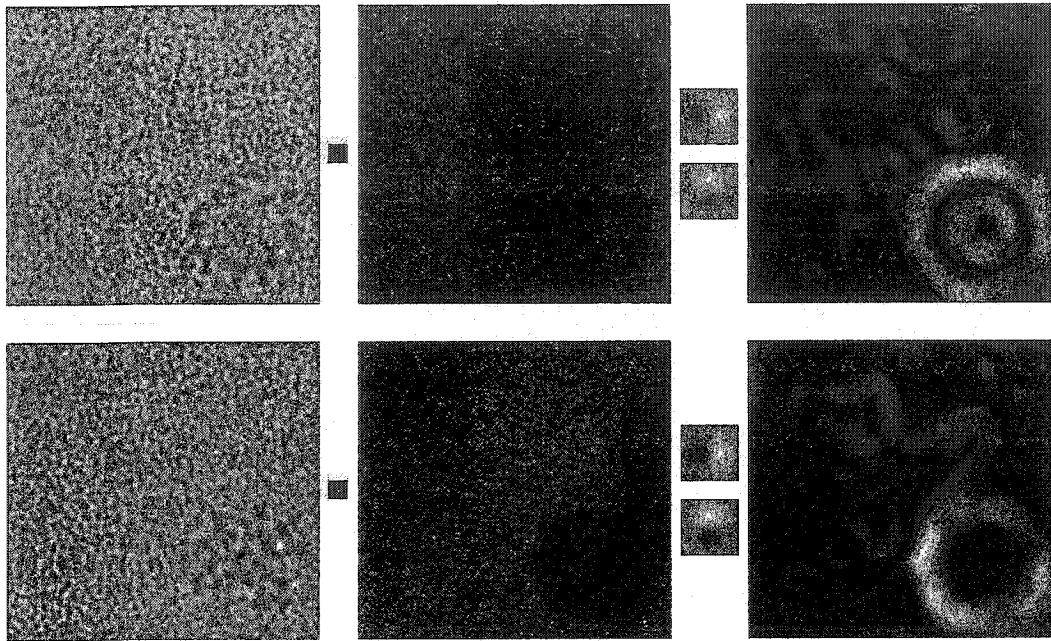


Figure 4.1 The first column shows the stimulus made of four quadrants with the disparate region in the lower-right quadrant. The disparate region was either an annulus or a circle with random filtered noise of lower spatial frequency than in the background. The second column shows the stimulus convolved with a Gaussian filter. This has the effect of separating the disparate region from the background. The third column shows the result of the convolution of the second column with a Laplacian of a Gaussian ($\nabla^2 G$ filter); the effect is to isolate the boundaries.

combining windowed samples of two textures (t_1 and t_2). A window (w) had values in the range $[0, 1]$.

$$\text{Stimulus} = (w * t_1)^{1/2} + ((1 - w) * t_2)^{1/2} \quad 4.1$$

In Low-in-High conditions the background texture (t_2) was fixed at 4.74 cpd and the disparate texture (t_1) took on one of the seven values from 3.65 to 4.74 cpd. In High-in-Low conditions the disparate texture was fixed at 4.74 cpd and the background frequency varied.

Procedure

The stimulus was viewed at a distance of 60 cm for 116 ms. In every other aspect the procedure was similar to preceding experiments

Results

Figure 4.2. and Table 4.1 summarize the results of Experiment 5. The data fitting procedure was as in previous experiments, i.e. with Weibull functions. A 2 x 2 within subjects ANOVA (Appendix 2) revealed that thresholds were significantly lower for circular regions ($F(1, 8) = 25.49, p < .001$). In addition, Low-in-High frequency stimuli had significantly lower thresholds than High-in-Low frequency stimuli ($F(1,8)=11.41, p < 0.01$). There was no significant interaction between boundaries and frequency asymmetries. These results show that circular regions were more salient than rings that had double of their boundary length and third of their area and Low-in-High frequencies are more salient than High-in-Low frequencies.

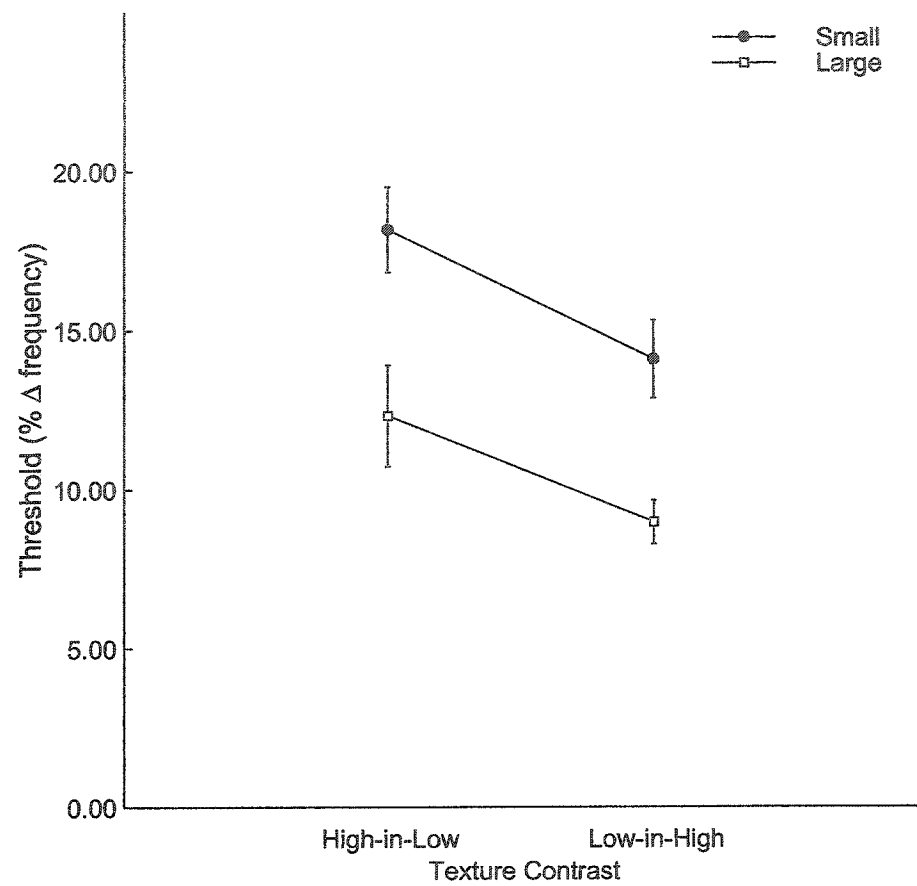


Figure 4.2 Summary of Experiment 5, ($n = 9$). Error bars represent \pm one *SEM*. The thresholds are always lower in the case of circles.

Table 4.1

*Weber fraction at 72 percent thresholds for random filtered noise textures:
the foreground is a ring (double edge) or a circle (simple edge)*

Participant	Double Edge		Simple Edge	
	High in low	Low in high	High in low	Low in high
MI	0.12	0.11	0.09	0.11
AP	0.23	0.11	0.12	0.07
CVD	0.14	0.15	0.09	0.08
FM	0.15	0.11	0.11	0.08
FS	0.21	0.18	0.15	0.13
GA	0.21	0.17	0.23	0.08
NW	0.23	0.20	0.11	0.07
RG	0.18	0.10	0.08	0.08
SM	0.16	0.14	0.14	0.10
mean	0.18	0.14	0.12	0.09
SEM	0.04	0.03	0.05	0.02

Discussion

Given our initial assumptions, the results suggested that texture discrimination was more affected by region properties than edge properties. Results also suggested that perceptual asymmetry existed as found by Gurnsey and Browse (1989), namely low frequency patches in a high frequency background, or in Gurnsey and Browse terms, large circles patches in small circles background, were more salient than high frequency patches in low frequency background. However, it did not matter if the patch was presented in circle or in ring form: the interaction was non significant. Consequently, this experiment could not be used to decide whether the asymmetry was done by an edge detection mechanism or a region detection mechanism.

To assess the assumption that discrimination was more affected by region properties, we implemented a back-pocket model (Chubb & Landy, 1991) of texture segmentation. The model comprised (i) convolution with a $\nabla^2 G$ filter, (ii) a squaring rectification and (iii) a gradient computation (see Figure 4. 1). The gradient was found by a convolution with two odd Gabors with perpendicular orientations (Figure 4.1). Decisions were made by (1) integrating the second layer responses or (2) integrating the first layer responses (results of convolution with a Gaussian) to represent edge and region based strategies, respectively. We simulated performance in a 2AFC and measured decrement conditions for both region types. Thresholds were determined as in the experiment. For the edge model we determined thresholds for different sizes of second layer filters. The results are shown in Figure 4.3.

The region based strategy shows an advantage of the circular window,

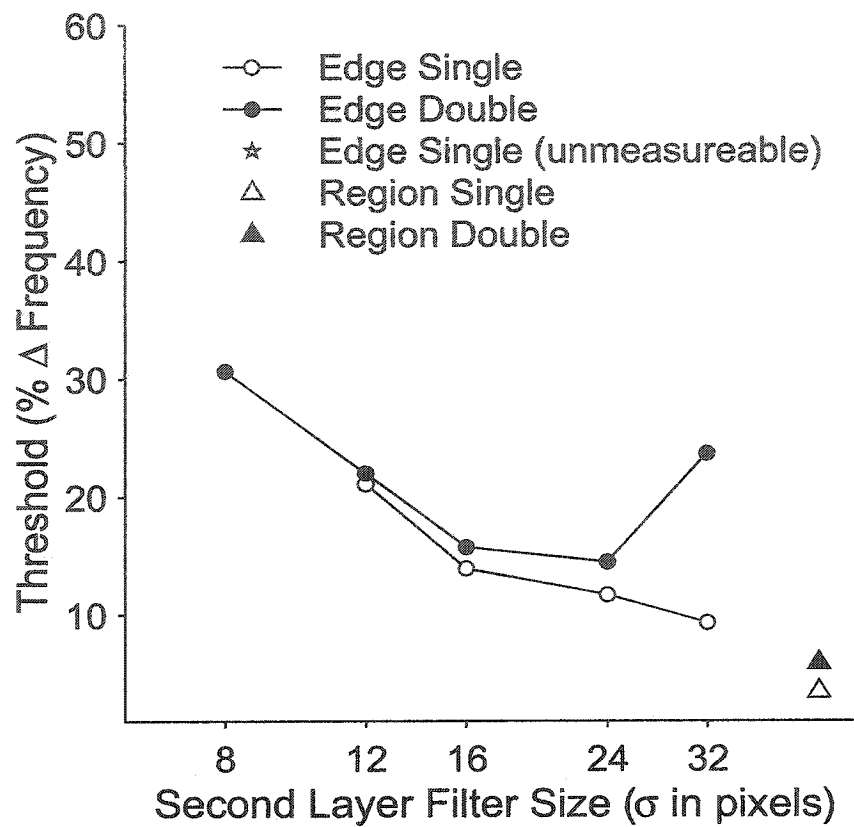


Figure 4.3 Simulated thresholds in responses to texture differences in circular (single edge) and annular (double edge) windows. Edge based thresholds are very similar for intermediate sizes of the second layer filter and diverge a very small and very large sizes. The region strategy shows an advantage for the single edge stimuli.

and if this model simulates correctly what happens in the visual system, the first stage is not influenced by the edges.

The edge strategies on the other hand show an advantage for the annular windows (double edge) at small second layer filters while at very low frequency filters they show an advantage of the circular (single edge). In the middle range, the filters have a similar effect. Therefore, as long as a boundary can be clearly identified, the second layer filters can deal with it by assigning the right frequency filter to the template. In the following paragraph we studied what happened when the boundary was hard to find.

4.3 Discrimination in Blurry Boundaries

The dichotomy between regions and edges can be understood in still another paradigm. Instead of increasing the length of the edges, one can dilute somehow the abruptness of edge (Figure 4.4.) and test how the discrimination will vary accordingly. The following experiment did just that. Assumptions were again that if discrimination depended on edges more than on regions, the steeper the edge the easier the discrimination.

Experiment 6

Method

Subjects.

Five participants were selected from the Psychology department at Concordia University. All reported normal to corrected-to-normal vision.

Stimuli.

Stimuli were created from seven texture arrays comprising isotropic, band pass noise having centre frequencies that ranged from 7.9 to 9.5 cpd in seven equal log steps. We used stimuli of the sort shown in Figure 4.4. The

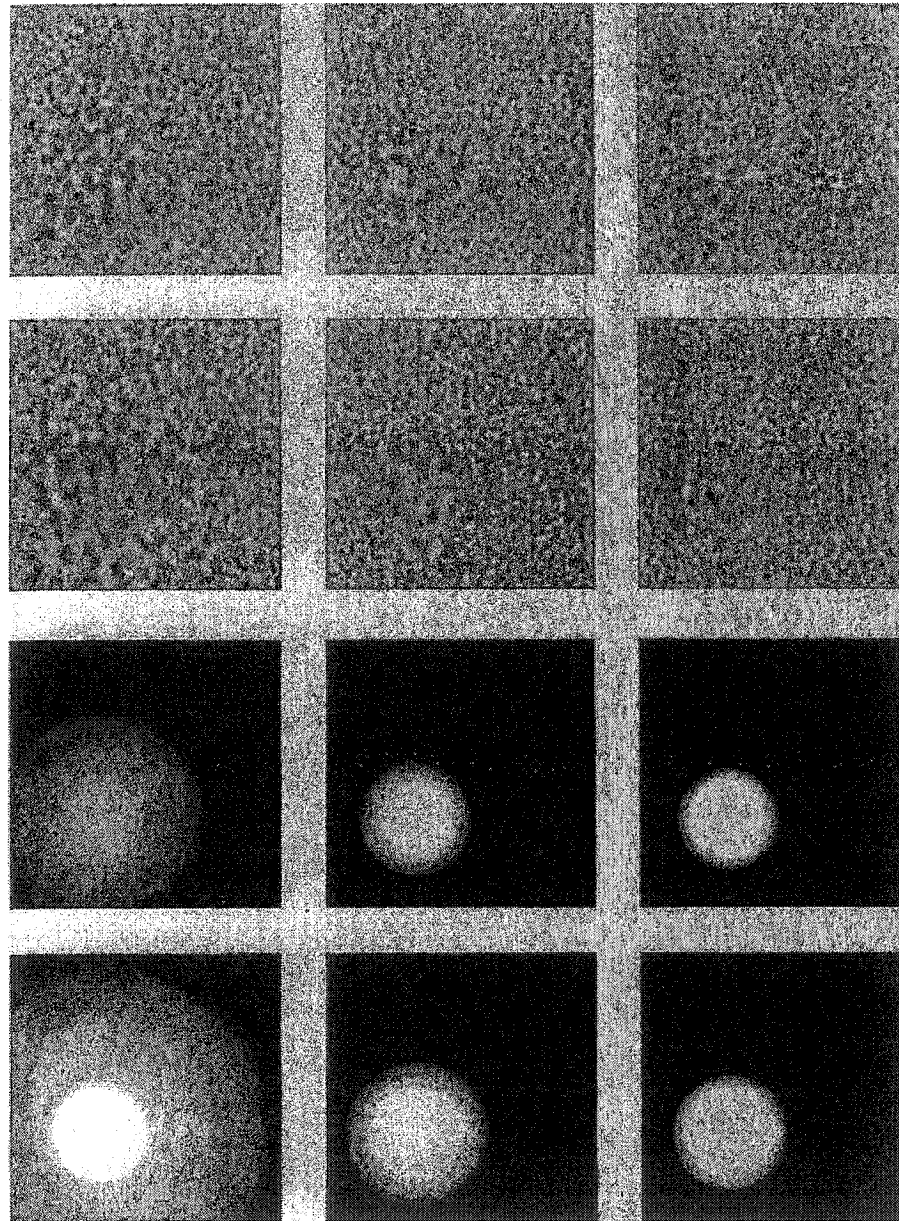


Figure 4.4 Stimuli with different edge slopes. The upper six panels show the actual stimuli, whereas the lower six panels show the slopes. The slopes always grow linearly and the proportion of each texture grows from zero to one. In the first and third rows the proportion reaches 0.5 at always the same distance, making the pure background texture centre smaller and smaller. In the second and fourth rows, it is the corona of blended mixtures that becomes larger and larger, the non blended centre keeps the same size.

stimuli varied in the abruptness (slope) of the transition from t_1 to t_2 . Slopes of 0.1, 0.05 and 0.01 indicate that the transition from t_1 to t_2 occurred over distances of 0.23, 0.46 and 2.29 degrees respectively. These slopes correspond to the left, centre and right columns of Figure 4.4 respectively. In the top three panels of Figure 4.4 the point at which the two textures were mixed in equal proportions (i.e., $w = 0.5$) occurs at the nominal width of the disparate texture region (4.75°). In the next three panels the point at which the two textures were mixed in equal proportions occurs at a distances of 0.11, 0.23 and 1.14° from the nominal width of the disparate region. (The top six panels represent example stimuli and the bottom six panels represent the windows used to create the stimuli).

Procedure

The procedure was identical to the previous experiment except that instead of 2x2 conditions there were 2x3 conditions represented by the top six panels of Figure 4.4.

Results

Table 4.2 and Figure 4.6 summarize the results of Experiment 6 found by Weibull function fitting. The data were submitted to a 2 (widths) by 3 (slopes) within subjects ANOVA. There was a main effect of slopes ($F(2, 8) = 7.66, p < .02$). The steeper the slope the lower the threshold, i.e. the more salient the foreground. The ANOVA showed also a trend toward a significant widths by slopes interaction ($F(2, 8) = 4.04, p < .1$). There was no main effect of width, but this may be attributable to the low power of the design.

Table 4.2

Weber fraction at 72 percent threshold for different slopes and different sizes of the centre.

size centre	sc=variable			sc=1		
	0.01	0.05	0.1	0.01	0.05	0.1
slope	0.01	0.05	0.1	0.01	0.05	0.1
participants						
SM	0.19	0.13	0.10	0.11	0.13	0.08
DV	0.14	0.13	0.09	0.12	0.12	0.08
FS	0.10	0.07	0.08	0.09	0.11	0.07
GR	0.11	0.07	0.06	0.10	0.08	0.07
N W	0.30	0.15	0.12	0.14	0.09	0.12
mean	0.17	0.11	0.09	0.11	0.11	0.08
SEM	0.08	0.04	0.02	0.02	0.02	0.02

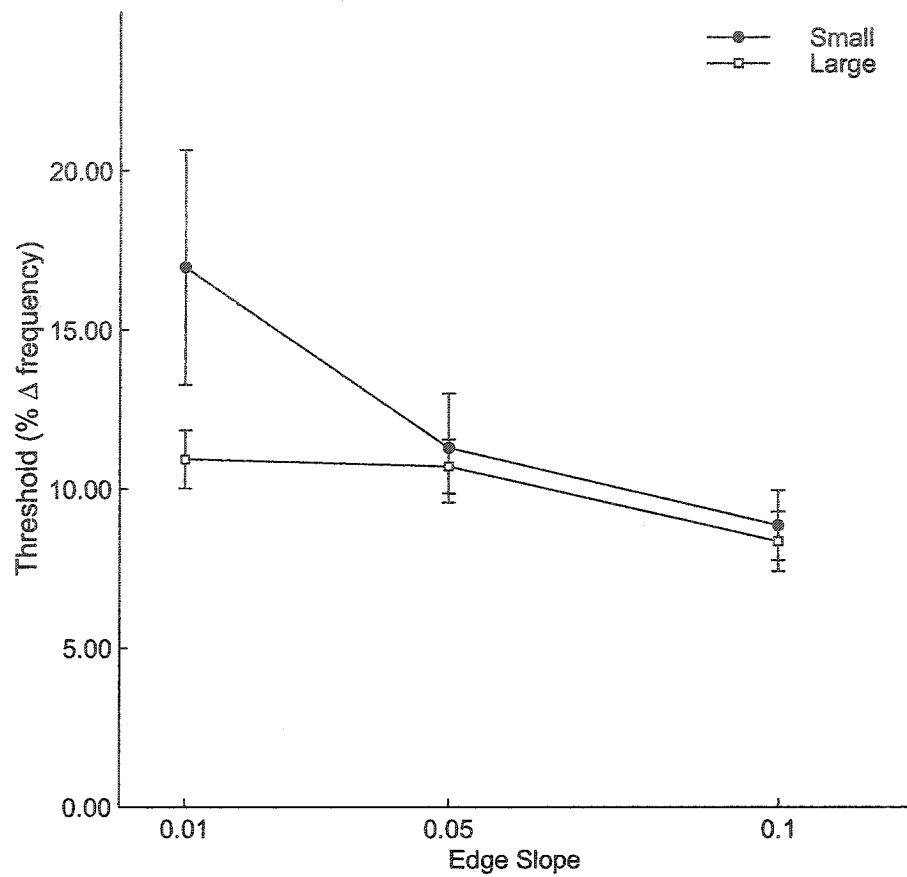


Figure 4.5 Summary of Experiment 2 ($n = 5$). Error bars represented \pm one SEM. The thresholds were in general lower (more salient) for the large uniform foreground even if the situation was more ambiguous with the medium edge slope, in which case neither the region theory nor the edge theory was telling the whole story. Small in the legend corresponds to the variable centre i.e. the first row in Figure 4.4. Large corresponds to the second row.

Discussion.

The results of Experiment 6 show a main effect of region type (annulus vs circle) which could be explained by the edge or region mechanisms described in Figure 4.2.

Edge and region responses were simulated in the same way as for Experiment 5 and the results are shown in Figure 4.6. Region responses were computed as before, and edge responses assumed a second layer filter having $\sigma = 16$ (see Figure 4.3). Thresholds were computed for Low-in-High conditions. There are qualitative similarities between the results of Experiment 6 and the two analyses shown in Figure 4.6. The experimental results show a main effect of slope that is generally consistent with the edge analysis shown

The results of Experiment 5 suggest that sensitivity is not based exclusively on edge or region sensitive mechanisms. However, a combination of these mechanisms might explain the data. The trend toward a region size effect may be explained by the region mechanism and the significant slope effect may be explained by an edge mechanism.

We conclude, as did Du Buf (1992) that the edge-based and the region-based mechanisms coexist and act in parallel.

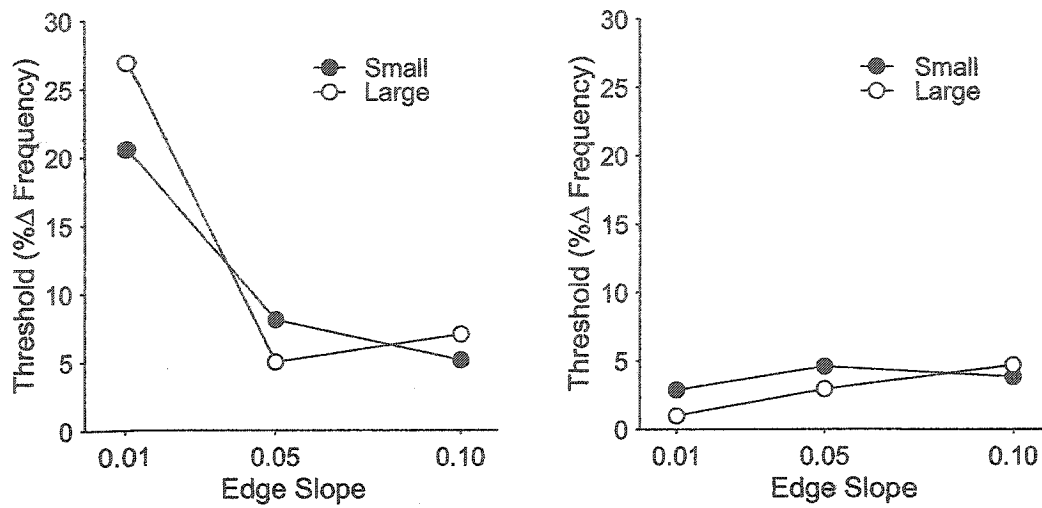


Figure 4.6 Simulated Low-in-High thresholds for the texture contrasts depicted in Figure 4.4. The left panel shows simulated thresholds for small (Figure 4.4, first row) and large (Figure 4.4, second row) regions as a function of slope based on an edge decision process. The right panel shows simulated thresholds based on a region decision process for the same conditions as a function of slope.

Chapter 5 General discussion

Numerous researchers have tried to explain texture discrimination but one or more aspects could not fit with their theories. One of the phenomena that resisted the inclusion in a complete theory of texture is the discrimination asymmetry. Some vision theorists like Malik and Perona (1990) for example acknowledged the failure of their model to explain the asymmetry. Liu and Wang (2002) were able to explain the asymmetry reported by Gurnsey and Browse (1987) but their model would not explain sensitivity to amplitude modulations as described by Kingdom and Keeble (2000).

This study focused on several aspects that influence the asymmetry of texture discrimination. Gurnsey and Browse (1987) and Rubenstein and Sagi (1990) suggested that variability of micropatterns might play a role. A simple implementation of the signal detection theory and the quadratic forms showed that this assumption was plausible and Experiment 1 with simple oriented lines showed a qualitative agreement to the model.

Gurnsey and Browse (1987, 1989) suggested also that the asymmetry might depend on the enclosing circles of the micropatterns. In Experiment 2 either stimuli were made of non rotated Vs and Xs or stimuli were made of randomly rotated Vs and Xs. The test was made with micropatterns varying from Vs to Xs or vice versa. In both cases Vs rotated or not had the same enclosing circles and Xs rotated or not had the same enclosing circles (Figure 3.2 and Figure 3.3). The variability showed a stronger influence on asymmetry than the enclosing circles because the asymmetry in the case of non varied Vs and Xs was minute. The influence of the enclosing circles was shown to be weak also in Experiment 5 with random filtered noise (Figure 4.1). Low frequency noise in a background of high frequency noise was significantly

more salient than high frequency noise in a background of low frequency noise.

The characteristics of the micropatterns showed that they could have an influence too. William and Julesz (1992b) demonstrated that the asymmetry could be reversed in certain conditions, for example by changing the position of the micropatterns. Experiment 3 looks like Experiment 2 except the micropatterns are larger and the foreground-background ratio is more important (Figures 3.6 and 3.7). As a result, the asymmetry was reversed (Xs more salient) and the influence of the enclosing size was significantly larger. But the reversal of asymmetry happened only with Vs and altered Vs (Xs) as shown in Figure 3.7. In Experiment 4, where X and altered X micropatterns were used, the asymmetry as found by Gurnsey and Browse (1987) was restored, Vs were more salient in Xs than vice versa. One explanation is that Vs and altered Vs are more different than Xs and altered Xs, indicating that textons too are playing a role in defining the asymmetry.

Rubenstein and Sagi (1990) and many researchers with them thought that the discrimination and therefore the asymmetry happened on the boundaries. However Gurnsey and Laundry (1992) showed that diluting the boundaries had little effect on asymmetry and discrimination. Experiment 5 tried to address this issue with stimuli made of filtered random noise and circular boundaries. One foreground was made of an annulus (double edge) and the other was made of a circle (simple edge), the first case had a larger boundary perimeter and a smaller area than the second. The larger area proved to be more salient indicating a region-based mechanism. However in Experiment 6 where the boundaries were gradually diluted (Figure 4.4) the results showed that edges played a more important role. Simulation of area-

based and edge-based mechanisms showed that both edges and regions seemed to take part in the texture discrimination.

One of the issues that remain to be addressed is the influence of the foreground-background area ratio. As shown in Experiment 3, it seems that at a certain point there is a figure-ground change that results in asymmetry reversal. Another interesting research question is the quantification of general textures as it was done in chapter 2 with quadratic forms in a way that would solve the problems of discrimination and asymmetry at the same time.

One promising challenge in texture segmentation and asymmetry would be to put together the Malik and Perona (1990) theory with its multiple filters and its two stages of rectification and the Liu and Wang (2002) theory with its possibility of asymmetry explanation and its backwards calculations from the filter results to the original image.

The most seductive idea in texture segmentation is to find a unification theory that would explain all the observed phenomena but this theory has been hard to find. It is still possible that a unique pathway does not exist. In other fields of nature, it has been found that some organisms have many different pathways to make the same proteins or at least roughly similar proteins so that when one pathway is knocked down the entity still survives on the backup systems (Shanks and Joplin, 1999). If the same complexity exists in texture vision, the understanding of the system might be blurred by the fact that at a certain point one pathway starts to interfere with other pathways, thus making really difficult the isolation of single systems.

References

- Bach, M. & Meigen, T. (1992). Electrophysiological correlates of texture segregation in the human visual evoked potential. *Vision research*, 32, 417-424.
- Barth, E., Zetzsche, C. & Rentschler, I. (1998). Intrinsic two-dimensional features as textons. *Journal of the Optical society of America, A*, 15, 1723-1732.
- Bergen, J. R. (1991). Theories of visual texture perception. In D. Regan, (Ed.), *Vision and visual dysfunction*, 10, 114-134.
- Buf du, J. M. H. (1992). Abstract processes in texture discrimination. *Spatial Vision*, 6, 221-242.
- Chubb, C. & Landy, M.S. (1991). Orthogonal distribution analysis: A new approach to the study of texture perception. In Landy, M. S. & Movshon, J. A. (Eds). *Computational models of visual processing*, 291-301. Cambridge, MA: The MIT Press.
- Egan, J.P. (1975). *Signal detection theory and ROC analysis*. New York: Academic press.
- Falmagne, J.-C. (1985). *Elements of psychophysical elements*. Toronto: Oxford University Press.
- Fogel, I. & Sagi, D. (1989). Gabor filters as texture discriminator. *Biological Cybernetics*, 61, 103-113.
- Goldstein, E. B. (1996). *Sensation & perception, 4h ed*. Toronto: Brooks/Cole Publishing company.
- Green, D. M. & Swets, J. A. (1966). *Signal detection theory and psychophysics*. New York: Wiley.
- Gurnsey, R. & Browse, R. A. (1987). Micropattern properties and presentation

- conditions influencing visual texture discrimination. *Perception & psychophysics*, **41**, 239-252.
- Gurnsey, R. & Browse, R. A. (1989). Asymmetries in visual texture discrimination. *Spatial Vision*, **4**, 31-44.
- Gurnsey, R. & Fleet, D. J. (2001). Texture space. *Vision Research*, **41**, 745-757.
- Gurnsey, R. & Laundry, D. S. (1992). Texture discrimination with and without abrupt texture gradient. *Canadian Journal of Psychology*, **46**, 306-332.
- Harvey, L. O. (1986). Efficient estimation of sensory thresholds. *Behavior Research Methods, Instruments & Computers*, **18**, 623-632.
- Harvey, L. O. & Gervais, M. J. (1978). Visual texture perception and Fourier analysis. *Perception & Psychophysics*, **26**, 534-543.
- Hubel, G. H. & Wiesel, T. N. (1959). Receptive fields of single neurons in the cat's striate cortex. *Journal of Physiology*, **148**, 574-591.
- Julesz, B. (1981). Textons, the elements of texture perception, and their interaction. *Nature*, **290**, 91-97.
- Julesz, B. (1986). Texton gradients: the texton theory revisited. *Biological cybernetics*, **54**, 245-251.
- Kastner, S., Nothdurft, H. C. & Pigarev, I. N. (1999). Neuronal responses to orientation and motion contrast in cat striate cortex. *Visual Neuroscience*, **16**, 587-600.
- Kingdom, F. A. A. & Keeble, D. R. T. (2000). Luminance spatial frequency differences facilitate the segmentation of superimposed textures. *Vision Research*, **40**, 1077-1087.
- Kröse, B. J. A. (1987). Local structure analyzers as determinants of preattentive pattern discrimination. *Biol. Cybern.*, **55**, 289-298.
- Landy, M. S. & Bergen, J. R. (1991). Texture segregation and orientation

- gradient. *Vision Research*, 31, 679-691.
- Liu, X. & Wang, D. (2002). A spectral histogram model for texton modeling and texture discrimination. *Vision Research*, 42, 2617-2634.
- Malik, J. & Perona, P. (1990). Preattentive texture discrimination with early vision mechanisms. *JOSA A*, 7, 923-932.
- Marr, D. (1982). *Vision*. New York. W.H.Freeman and Company.
- Mathai, A.M. & Provost, S.B. (1992). *Quadratic forms in random variables*. New York.Marcel Dekker Inc.
- Nothdurft, H. C. (1985). Sensitivity for structure gradient in texture discrimination tasks. *Vision Research*, 25, 1957-1968.
- Nothdurft, H. C., Gallant, J. L. & Van Essen, D. C. (2000). Response profiles to texture border patterns in area V1. *Visual Neuroscience*, 17, 421-436.
- Popple, A. (2003). Context effects on texture border localization bias. *Vision Research*, 43, 739-743.
- Rosenholtz, R. (2001). Search asymmetries? What search asymmetries? *Perception & Psychophysics*, 63, 476-489.
- Rubenstein, B. S. & Sagi, D. (1990). Spatial variability as a limiting factor in texture discrimination tasks: implications for performance asymmetries. *J.O.S.A. A*, 7, 1632-1643.
- Sezikeye, F.X. & Gurnsey, R. (2003, May). Texture regions are more easily detected than texture edges. Poster session presented at the annual meeting of the Vision Science Society, Sarasota, FL.
- Shanks, N. & Joplin, K. H. (1999). Redundant complexity: a critical analysis of intelligent design in biochemistry. *Philosophy of Science*, 66, 268-282.
- Tonder, G.J. van & Ejima, Y. (2000a). From image segmentation to anti-textons. *Perception*, 29, 1231-1247.

- Tonder, G.J. van & Ejima, Y. (2000b). The patchwork engine: image segmentation from shape symmetries. *Neural networks*, **13**, 291-303.
- Treisman, A. (1985). Preattentive processing in vision. *Computer vision, graphics, and image processing*, **31**, 156-177.
- Treisman, A. & Gormican, S. (1988). Feature analysis in early vision: evidence from search asymmetry. *Psychological Review*, **95**, 15-48.
- Wertheimer, M. (1923/1958). Principles of perceptual organization. In D. C. Beardslee & M. Wertheimer, (eds), *Readings in perception*, 115-135. Princeton: D. Van Nostrand Company, Inc.
- Wilkinson, F. (1995). Acuties for textures and gratings in kittens assessed by preferential looking. *Behavioural-Brain-Research*. **68**, 185-199.
- Williams, D. & Julesz, B. (1992a). Perceptual asymmetry in texture perception. *Proc. Natl. Acad. Sci. USA*, **89**, 6531-6534.
- Williams, D. & Julesz, B. (1992b). Filters versus textons in human and machine texture discrimination. In H. Wechsler (ed.). *neural networks for perception: human and machine perception*. Vol. 1, 145-175. NewYork: Academic Press.
- Wolfson, S. S. & Landy, M. S. (1998). Examining edge- and region-based texture analysis mechanisms. *Vision Research*, **38**, 439-446.
- Zar, J. H. (1984). *Biostatistical analysis, 2nd edition*. Englewood Cliffs, N.J.: Prentice-Hall, Inc.
- Zetzsche C. & Barth, E. (1990). Fundamental limits of linear filters in the visual processing of two-dimensional signals. *Vision Research*, **30**, 1111-1117.

Appendix 1

Analysis of Variance for Asymmetric Discrimination between Ls and Xs

Source	df	F	h2	p
Foreground (F)	1	49.225	.908	.001**
Orientation (O)	1	8.615	.633	.032*
F x O	1	.110	.022	.754
Within group error	4			

**statistically significant results at $p < .01$, *statistically significant results at $p < .05$.

Appendix 2

Within subject contrasts ANOVA, Circles vs annulus, High frequency background vs low frequency background

Source	df	F	η^2	p
Form of disp. region	1	25.49	0.76	0.001**
Bg spatial freq	1	11.41	0.59	0.01**
Bsf x Fdr	1	0.06	0.01	0.81
within group error	8			

**statistically significant results at $p < .01$.